THE ASTRONOMICAL JOURNAL, 122:1030–1050, 2001 August

NONLINEAR CORE-MANTLE COUPLING

JIHAD TOUMA
Department of Physics and Center for Advanced Mathematical Sciences, American University of Beirut,
P.O. Box 11-0236, Beirut, Lebanon; jt00@aub.edu.lb

AND

JACK WISDOM
Department of Earth, Atmospheric, and Planetary Sciences, Massachusetts Institute of Technology,
77 Massachusetts Avenue, Cambridge, MA 02139; wisdom@mit.edu
Received 2000 September 11; accepted 2001 April 26

ABSTRACT

We explore the nonlinear dynamics of a forced core-mantle system. We show that the free axisymmetric motion of a uniform-vorticity fluid core coupled to a rigid mantle (the Poincaré-Hough model) is integrable. We derive an approximate Hamiltonian for the core tilt mode that includes the leading nonlinear contribution. We then include gravitational perturbations in the analysis. We identify the principal nonlinear prograde and retrograde resonances and the characteristic excitation associated with each. We compare the nonlinear excitation with the excitation expected in the corresponding linear model. The nonlinear model indicates that for each principal commensurability there are multiple overlapping resonances, and so varying degrees of chaotic behavior are predicted. Chaotic behavior at the principal core-mantle commensurabilities is confirmed with surfaces of section. We then present the results of numerical evolutions done with a generalization of our (1994) Lie-Poisson integrator to allow for a Poincaré-Hough core, core-mantle friction, and tidal dissipation. We use our analytical and numerical models to explore the evolution of Earth through the prograde core-mantle resonances and to explore the evolution of Venus through the retrograde resonances. Heating of the core-mantle boundary during resonance passage is much greater for Venus than for Earth. We raise the question whether heating during core-mantle resonance passage could be responsible for the global resurfacing of Venus.

Key words: celestial mechanics — Earth — methods: numerical — planets and satellites: individual (Venus) — solar system: general

1. INTRODUCTION

Gravitational torques from the Sun and Moon induce nutational and precessional motions of the solid Earth. These motions couple to Earth's fluid core and excite fluid flow via conservative pressure and viscous torques at the core-mantle interface. This flow, if and when substantial, could play an important role in the energy balance of the planet. Our work is concerned with the investigation, in a nonlinear Hamiltonian framework, of the dynamics of this astronomically forced, coupled core-mantle system.

Toomre (1974) observed that roughly 200 million years ago Earth must have passed through a resonance between the precession of the core vorticity and Earth yearly nutation. A number of other authors have picked up on this and noted the near-coincidence of such a resonance with the Permo-Triassic extinction. Hinderer, Legros, & Amalvict (1987) examined, in a linear model, the nature of these resonances and the magnitude of the response when an account is made of the elastic deformation of the planet and dissipation. More recently, Williams (1994) reconsidered the problem. Williams placed the main annual resonance 500–570 million years ago and prefers to link its effect to other geophysical events. Greff-Lefftz & Legros (1999) revisited earlier calculations, including the effects of the inner core, and estimated the epochs of resonance passage. They found that the annual resonance passage occurred about 270 million years ago and that 5×10^{25} joules are deposited at the base of the mantle during resonance passage. They assert that this heat destabilizes the D'' layer, leading about 20 million years later to mantle plumes that could be responsible for continental flood basalt volcanism (the Siberian traps, 250 Myr ago). They correlate dates of occurrence of other resonances with crust-forming episodes.

The surface of Venus is geologically young. The crater age is estimated to be in the range 700–800 million years (McKinnon et al. 1997). A widely accepted interpretation is that Venus has undergone a global volcanic resurfacing (Schaber et al. 1992; Strom, Schaber, & Dawson 1994). We raise the question whether the global resurfacing of Venus might be a consequence of resonant heating resulting from passage through a core-mantle resonance. As we show below, as a consequence of the retrograde rotation of Venus the core-mantle resonances are much stronger for Venus than for Earth. Perhaps the heating is sufficient to initiate a global resurfacing of Venus, and the less intense heating of Earth is responsible for the Siberian traps? A simple matter of the direction of the rotation might thus account for the dramatic differences in the surface and atmospheric states of Earth and Venus.

We present here our investigations of the tidal evolution of Earth and Venus through these core-mantle resonances. Our work builds on our earlier investigations of the nonlinear dynamics of spin-orbit coupling in the solar system. These investigations include the extension of the symplectic n-body mapping method of Wisdom & Holman (1991) to handle rigid-body dynamics (Touma & Wisdom 1994a, hereafter TW94a), the discovery of the chaotic obliquity of Mars (Touma & Wisdom 1993), application of modern numerical and Hamiltonian methods to a reexamination of the tidal history of the Earth-Moon system (Touma & Wisdom 1994b), and the discovery of a possible explanation of the mutual inclination of the Moon (Touma & Wisdom

1998). In this work, we build on these investigations to examine the passage of Earth and Venus through the various nonlinear core-mantle resonances. We investigate the nonlinear dynamics of resonances in the astronomically forced core-mantle system. We find that for Venus there are significant chaotic zones near resonance; for Earth there are smaller chaotic zones. We study the tidal evolution through the core-mantle resonances with both approximate resonance models and full numerical simulations. The full simulations uncover processes that can have a dramatic effect on the amount of heat deposited during resonance passage.

2. HAMILTONIAN FORMULATION

We start by giving a Hamiltonian formulation of the Poincaré-Hough equations (Hough 1895; Poincaré 1910; Lamb 1945). These equations describe the motion of a rigid mantle with a triaxial ellipsoidal cavity filled with inviscid fluid. The fluid is assumed to have uniform vorticity; this amounts to assuming that only the first Hough mode is active. The fluid is assumed to have constant uniform density.

The components (u, v, w) of the velocity field of the fluid on the mantle's principal axes are

$$u = (a/c)q_c z - (a/b)r_c y + qz - ry , \tag{1}$$

$$v = (b/a)r_c x - (b/c)p_c z + rx - pz , \tag{2}$$

$$w = (c/b)p_c y - (c/a)q_c x + py - qx , \tag{3}$$

where (x, y, z) are the mantle components of the position vector and a, b, and c are the principal elliptical radii of the cavity. The mantle components of the angular velocity of the mantle are (p, q, r). The parameters p_c, q_c, and r_c specify the velocity field of the fluid; for a spherical cavity, these become the angular velocity of the core relative to the mantle. This velocity field exactly satisfies Helmholtz's equations.

The kinetic energy T of the system is obtained by integration:

$$2T = Ap^2 + Bq^2 + Cr^2 + A_c p_c^2 + B_c q_c^2 + C_c r_c^2 + 2F_c pp_c + 2G_c qq_c + 2H_c rr_c , \tag{4}$$

where A, B, and C are the principal moments of inertia of the whole body and A_c, B_c, C_c, F_c, G_c, and H_c are parameters for the core. For a uniform-density fluid in an elliptical cavity, we have

$$A_c = \tfrac{1}{5}M_c(b^2 + c^2), \quad B_c = \tfrac{1}{5}M_c(c^2 + a^2) , \quad C_c = \tfrac{1}{5}M_c(a^2 + b^2) , \tag{5}$$

$$F_c = \tfrac{2}{5}M_c bc, \quad G_c = \tfrac{2}{5}M_c ac, \quad H_c = \tfrac{2}{5}M_c ab , \tag{6}$$

where M_c is the mass of the core and A_c, B_c, and C_c are the principal moments of inertia of the core.

By integration, the mantle components (P, Q, R) of the angular momentum of the whole system are

$$P = Ap + F_c p_c = \frac{\partial T}{\partial p} , \quad Q = Bq + G_c q_c = \frac{\partial T}{\partial q} , \quad R = Cr + H_c r_c = \frac{\partial T}{\partial r} . \tag{7}$$

We define

$$P_c = \frac{\partial T}{\partial p_c} = F_c p + A_c p_c, \quad Q_c = \frac{\partial T}{\partial q_c} = G_c q + B_c q_c , \quad R_c = \frac{\partial T}{\partial r_c} = H_c r + C_c r_c . \tag{8}$$

The components (P_c, Q_c, R_c) have dimensions of angular momentum, but they are not components of the core angular momentum. Nevertheless, we sometimes refer to them as components of the core angular momentum for lack of a better name. Note the inverse relations

$$p = \frac{A_c P - F_c P_c}{\alpha} , \quad p_c = \frac{AP_c - F_c P}{\alpha} , \tag{9}$$

$$q = \frac{B_c Q - G_c Q_c}{\beta} , \quad q_c = \frac{BQ_c - G_c Q}{\beta} , \tag{10}$$

$$r = \frac{C_c R - H_c R_c}{\gamma} , \quad r_c = \frac{CR_c - H_c R}{\gamma} , \tag{11}$$

with $\alpha = AA_c - F_c^2$, $\beta = BB_c - G_c^2$, and $\gamma = CC_c - H_c^2$.

The Poincaré-Hough equations of motion are

$$\frac{d}{dt}P - rQ + qR = T_a , \quad \frac{d}{dt}P_c + r_c Q_c - q_c R_c = 0 , \tag{12}$$

$$\frac{d}{dt}Q - pR + rP = T_b , \quad \frac{d}{dt}Q_c + p_c R_c - r_c P_c = 0 , \tag{13}$$

$$\frac{d}{dt}R - qP + pQ = T_c , \quad \frac{d}{dt}R_c + q_c P_c - p_c Q_c = 0 , \tag{14}$$

where (T_a, T_b, T_c) are mantle components of the applied torque on the whole body.

These equations can be put into Lie-Poisson form (Poincaré 1910). Let $\boldsymbol{M}$ be the vector total angular momentum, with mantle components (P, Q, R), and $\boldsymbol{M}_c$ be the vector with mantle components (P_c, Q_c, R_c). Then the equations of motion, without external torques, can be written simply

$$\frac{d\boldsymbol{M}}{dt} = \boldsymbol{M} \times \nabla_{\boldsymbol{M}} H_{\rm CM} , \quad \frac{d\boldsymbol{M}_c}{dt} = -\boldsymbol{M}_c \times \nabla_{\boldsymbol{M}_c} H_{\rm CM} \tag{15}$$

with core-mantle Hamiltonian $H_{\rm CM} = T$ written in terms of the components (P, Q, R) and (P_c, Q_c, R_c):

$$H_{\rm CM} = \frac{1}{2\alpha}(A_c P^2 + AP_c^2 - 2F_c PP_c) + \frac{1}{2\beta}(B_c Q^2 + BQ_c^2 - 2G_c QQ_c) + \frac{1}{2\gamma}(C_c R^2 + CR_c^2 - 2H_c RR_c) . \tag{16}$$

In this form, we see that the magnitude of the total angular momentum, the magnitude of $\boldsymbol{M}_c$, and the energy are all conserved.

The Lie-Poisson form inspires a Hamiltonian formulation, with canonical coordinates and momenta that are similar to the Andoyer variables (Andoyer 1923). The canonical momenta are F, the component of the total angular momentum on the inertial z-axis; G, the magnitude of the total angular momentum; L, the component of the

total angular momentum on the Z body axis; and S, the component of $\boldsymbol{M}_c$ on the Z body axis. We take the body axes to be aligned with the ellipsoid axes; along body axes X, Y, and Z, the radii of the core are a, b, and c, respectively. The conjugate coordinates are f, the angle from the inertial x-axis to the ascending node of the plane perpendicular to the total angular momentum vector on the x-y inertial plane; g, the angle between the last node and the ascending node of the body X-Y plane on the plane perpendicular to the total angular momentum; l, the angle between the last node and the X body axis; and finally s, the angle between the X body axis and the ascending node of the plane perpendicular to the vector $\boldsymbol{M}_c$ on the body X-Y plane. The angles l and s are coplanar. Momentum variables are denoted by uppercase letters, and the conjugate coordinates are denoted by the corresponding lowercase letter. In terms of these canonical coordinates and momenta, we have

$$P = (G^2 - L^2)^{1/2} \sin l\,, \quad P_c = (N^2 - S^2)^{1/2} \sin s\,,$$
$$Q = (G^2 - L^2)^{1/2} \cos l\,, \quad Q_c = -(N^2 - S^2)^{1/2} \cos s\,,$$
$$R = L\,, \quad R_c = S\,, \tag{17}$$

where N is the conserved magnitude of $\boldsymbol{M}_c$. It is straightforward to verify that Hamilton's equations are equivalent to the Lie-Poisson equations. The Hamiltonian is $H_{\rm CM}$ reexpressed in terms of the canonical coordinates and momenta. We will not write the Hamiltonian explicitly, but we note that f, g, and F do not appear, and therefore F, G, and f are conserved quantities. These correspond to the fact that the total angular momentum is conserved and the orientation of the angular momentum is fixed in space. There are two nontrivial degrees of freedom.

At this point we specialize to the case in which the mantle and the core cavity are axisymmetric: $A = B$, $A_c = B_c$, $F_c = G_c$, $H_c = C_c$, and $\alpha = \beta$. The Hamiltonian is

$$H_{\rm CM} = \frac{1}{2\alpha}\left[A_c(G^2 - L^2) + A(N^2 - S^2)\right] + \frac{1}{2\alpha}\left[2F_c(G^2 - L^2)^{1/2}(N^2 - S^2)^{1/2} \cos (l + s)\right] + \frac{1}{2\gamma}\left[C_c L^2 + CS^2 - 2C_c LS\right]. \tag{18}$$

The coordinate angles appear in only one combination: $l + s$. A canonical transformation can be made so that this combination is one of the new variables. We then find that $L - S$ is a conserved quantity. The essential dynamics is reduced to a problem with one degree of freedom, so the axisymmetric core-mantle problem is integrable, a result that was known to Poincaré (1910) from a Lagrangian point of view.

Getino (1995a) has also presented a Hamiltonian formulation of the axisymmetric core-mantle problem. The approach is quite different from that presented here. The resulting Hamiltonian differs from that of equation (18) by terms of order the core flattening. Our Hamiltonian is exact for the Poincaré-Hough model; the approach of Getino may be easier to generalize to more realistic models.

3. NONLINEAR MODES

The equations of motion derived directly from the free core-mantle Hamiltonian (eq. [18]) are singular for small offsets of the spin axes of the core and mantle from the symmetry axis. A more convenient set of coordinates is now introduced, by a pair of canonical transformations.

The first transformation gives new momenta that are differences of the old momenta. We choose the generating function

$$F_2 = F'f + G'(f + g) + L'(f + g + l) + (N - S')(f + g + l + s)\,, \tag{19}$$

giving $F' = F - G$, $G' = G - L$, $L' = L - S$, and $S' = N - S$, with conjugate angles $f' = f$, $g' = f + g$, $l' = f + g + l$, and $s' = -(f + g + l + s)$. The inverse relations are $S = N - S'$, $L = L' + N - S'$, $G = G' + L' + N - S'$, $F = F' + G' + L' + N - S'$, $f = f'$, $g = g' - f'$, $l = l' - g'$, and $s = -s' - l'$. Note that the new angles all have a common inertial reference. The momentum G' is small (and positive) if the total angular momentum is nearly aligned with the body symmetry axis; the momentum S' is small (and positive) if the core angular momentum is nearly aligned with the symmetry axis. In terms of the new variables, the Hamiltonian is

$$H_{\rm CM} = \frac{1}{2\alpha}\left\{A_c G'[G' + 2(L' - S' + N)] + AS'(2N - S')\right\} + \frac{1}{2\alpha}\left(2F_c\{G'[G' + 2(L' - S' + N)] \times S'(2N - S')\}^{1/2} \cos (g' + s')\right) + \frac{1}{2\gamma}\left\{C_c(L' - S' + N)^2 + C(N - S')^2 - 2C_c(L' - S' + N)(N - S')\right\}. \tag{20}$$

Note that the variable l' is not present, so the conjugate momentum $L' = L - S$ is an integral.

Next we make the canonical transformation

$$x = \sqrt{2G'} \cos g'\,, \quad y = \sqrt{2G'} \sin g'\,,$$
$$\xi = \sqrt{2S'} \cos s'\,, \quad \eta = \sqrt{2S'} \sin s'\,, \tag{21}$$

where x and ξ are the momenta conjugate to the coordinates y and η, respectively. The Hamiltonian is obtained by substitution. These variables are small when the momenta are nearly aligned with the symmetry axis, and the equations of motion in these variables are not singular there.

Next consider the "linearized" problem: we keep only the terms in the Hamiltonian that are quadratic in the variables x, y, ξ, and η. The equations of motion are linear in these variables. Ignoring the leading terms that do not depend on x, y, ξ, or η, this linearized Hamiltonian is

$$H_L = h_1\left(\frac{x^2 + y^2}{2}\right) + h_2(x\xi - y\eta) + h_3\left(\frac{\xi^2 + \eta^2}{2}\right) \tag{22}$$

with constants

$$h_1 = \frac{A_c}{\alpha}(L' + N), \quad h_2 = \frac{F_c}{\alpha}[(L' + N)N]^{1/2}\,,$$
$$h_3 = \left(\frac{A}{\alpha} + \frac{C_c - C}{\gamma}\right)N\,. \tag{23}$$

Note that $L' + N$ is approximately the total angular momentum.

The normal modes can be found by performing a canonical transformation that diagonalizes the Hamiltonian. The generating function of the transformation is

$$F_2 = \frac{y + c\eta}{\sqrt{D}} x_1 + \frac{cy + \eta}{\sqrt{D}} x_2 \tag{24}$$

with $D = 1 - c^2$, and c will be determined by the constraint that the Hamiltonian be diagonal. The new momenta and conjugate coordinates are x_i and y_i, respectively. The transformation of variables is

$$x = \frac{x_1 + cx_2}{\sqrt{D}}, \quad y = \frac{y_1 - cy_2}{\sqrt{D}},$$
$$\xi = \frac{cx_1 + x_2}{\sqrt{D}}, \quad \eta = \frac{-cy_1 + y_2}{\sqrt{D}}, \tag{25}$$

with similar equations for the inverse transformation. Substituting, the linearized core-mantle Hamiltonian becomes

$$H_L = \left(\frac{x_1^2 + y_1^2}{2}\right)\left(\frac{h_1 + 2h_2 c + h_3 c^2}{D}\right) + (x_1 x_2 - y_1 y_2)\left[\frac{(h_1 + h_3)c + h_2(1 + c^2)}{D}\right] + \left(\frac{x_2^2 + y_2^2}{2}\right)\left(\frac{h_1 c^2 + 2h_2 c + h_3}{D}\right), \tag{26}$$

and thus the condition for the Hamiltonian to be diagonalized is

$$(h_1 + h_3)c + h_2(1 + c^2) = 0 . \tag{27}$$

This is a quadratic equation for c. The roots are inverses of each other; we choose the root with magnitude less than 1 so that $(1 - c^2)^{1/2}$ is real. With this c, the linearized Hamiltonian is

$$H_L = \omega_1\left(\frac{x_1^2 + y_1^2}{2}\right) + \omega_2\left(\frac{x_2^2 + y_2^2}{2}\right) = \omega_1 \Theta_1 + \omega_2 \Theta_2 , \tag{28}$$

using the canonical transformation $x_i = (2\Theta_i)^{1/2} \cos\theta_i$, $y_i = (2\Theta_i)^{1/2} \sin\theta_i$. There are two uncoupled modes, with frequencies

$$\omega_1 = \frac{h_1 + 2h_2 c + h_3 c^2}{D}, \quad \omega_2 = \frac{h_1 c^2 + 2h_2 c + h_3}{D} . \tag{29}$$

The angles θ_i move uniformly with frequencies ω_i.

We define the dynamical flattening parameter $f = (C - A)/C$ and the core flattening parameter $f_c = (C_c - A_c)/C_c$. To first order in the flattening parameters, we have

$$c \approx \sqrt{\delta}(f_c - 1) , \tag{30}$$

where $\delta = C_c/C$. Note that c is negative. The frequencies are approximately

$$\omega_1 \approx \omega\left(1 + f\frac{C}{C_m}\right), \quad \omega_2 \approx \omega f_c \frac{C}{C_m}, \tag{31}$$

where ω is the rotational frequency and $C_m = C - C_c$ is the mantle moment of inertia. The first mode is a wobble mode; it is analogous to the wobble of a rigid body, but with the period in the body frame reduced by a factor C_m/C. The period of the Chandler wobble is reduced by the presence of a liquid core (see Hough 1895). (The period of the Chandler wobble is increased by the elasticity of the mantle; we do not consider effects of elasticity here.) We refer to the second mode as the "tilt" mode; it has a frequency that is proportional to the core flattening.

We now interpret the tilt mode in terms of the other variables. We assume that the amplitude of the wobble mode is zero: $x_1 = y_1 = 0$, so $\Theta_1 = 0$. We simplify the notation with $\Theta = \Theta_2$ and $\theta = \theta_2$. The motion in the (x_2, y_2)-plane is counterclockwise circular, with radius $(2\Theta)^{1/2}$. With no wobble, the motion in both the (ξ, η)- and (x, y)-planes is also circular, with radii $(2S')^{1/2}$ and $(2G')^{1/2}$, respectively. In this case, we have $G' = (c^2/D)\Theta$ and $S' = (1/D)\Theta$. Recall that $D = 1 - c^2$ and $c^2 \approx \delta(1 - 2f_c)$, to first order in the flattening parameters. Thus, $G' = c^2 S' \approx \delta(1 - 2f_c)S'$. Let J denote the angle between the total angular momentum and the symmetry axis; then $\cos J = L/G$, and

$$\sin^2 J = 1 - \frac{L^2}{G^2} \approx \frac{2G'}{L + N} , \tag{32}$$

where the approximation is for small J. Using $L' + N \approx C\omega$, we find

$$G' \approx \tfrac{1}{2} C\omega \sin^2 J . \tag{33}$$

Referring to equations (25), we see that if motion in the (x_2, y_2)-plane is counterclockwise, then the motion in the (x, y)-plane is clockwise and the motion in the (ξ, η)-plane is counterclockwise. Thus g' decreases, while s' increases, both with the tilt-mode frequency. Recall that g' measures the direction of the mantle symmetry axis in inertial space. The fact that g' decreases means that the body symmetry axis regresses about the total angular momentum. The angle between the symmetry axis and the angular momentum vector is J. Now, s' is related to the direction of the core angular momentum; s' increases, but because of the minus sign in its definition, this means the angular momentum of the core also regresses about the total angular momentum vector. The body symmetry axis and the core angular momentum both regress at the tilt-mode frequency. The body symmetry axis and the core angular momentum vector are coplanar with the total angular momentum; the total angular momentum is between them. Let K be the angle between the core angular momentum vector and the body symmetry axis. Then

$$\sin^2 K = 1 - \frac{S^2}{N^2} \approx \frac{2S'}{N} , \tag{34}$$

where the approximation is for small S'. So we have

$$S' \approx \tfrac{1}{2}\delta C\omega \sin^2 K . \tag{35}$$

Now $G' \approx \delta(1 - 2f_c)S'$, so we deduce

$$J \approx \delta(1 - f_c)K \tag{36}$$

for small J, K, and f_c. The angular offset of the body from the angular momentum vector is smaller than the angular offset of the core angular momentum vector from the symmetry axis by about a factor of δ, which is C_c/C.

We need the first nonlinear correction to the tilt-mode frequency. If we represent the frequency of the tilt mode as $\omega_2'(\Theta) = \omega_2 + k\Theta + \cdots$, we find, after some algebra,

$$k = \frac{A_c c^2(c^2-2) - A}{\alpha D^2} + \frac{C - C_c}{\gamma D^2} + \frac{F_c c[(c^2-2)N - (L'+N)]}{\alpha D^2[(L'+N)N]^{1/2}} . \quad (37)$$

Approximating $L' + N$ by $G = C\omega$ and N by $C_c\omega$, this becomes, to first order in the flattening parameters,

$$k = -\frac{f_c}{\delta C}\left[\frac{1 - 2\delta^2 + \delta^3}{(1-\delta)^3}\right]. \quad (38)$$

Note that the nonlinearity is large for both small core and large core. Also note that the nonlinearity is not dependent on the rotational frequency, except indirectly through the flattening. Thus, an approximate nonlinear Hamiltonian governing the tilt mode, assuming that the amplitude of the wobble mode is zero, is

$$H_T(\Theta) = \omega_2\,\Theta + \tfrac{1}{2}k\Theta^2 . \quad (39)$$

4. PERTURBATIONS

We consider gravitational perturbations from the Sun. Let m be the total mass of the planet with coupled core-mantle system, R the equatorial radius of the planet, and J_2 the gravitational quadrupole factor. We continue to specialize to an axisymmetric planet. Also, let M_S be the mass of the Sun and r be the Earth-Sun distance. The contribution to the potential energy from the second-order moments is

$$V_2 = \frac{GmM_S}{r}\frac{R^2}{r^2} J_2 P_2(\cos\theta_S) , \quad (40)$$

where G is the gravitational constant and θ_S is the angle from the symmetry axis to the Sun.

We reexpress the perturbation in terms of the core-mantle canonical coordinates. Let the position of the Sun be specified by distance r and true longitude λ. The two angles I and J satisfy $\cos J = L/G$ and $\cos I = F/G$. The angle I is the angle between the total angular momentum of the core-mantle system and the inertial z-axis; I is a measure of the obliquity of the planet. The angle J is the angle between the total angular momentum of the core-mantle system and the body symmetry axis and is a measure of the amplitude of the tilt mode (presuming the wobble mode has zero amplitude). The symmetry axis is brought from being initially parallel to the inertial z-axis to its actual position by a sequence of active rotations. Let $R_z(\theta)$ be an active right-hand rotation about the inertial z-axis by the angle θ and $R_x(\theta)$ be an active right-hand rotation about the inertial x-axis by the angle θ. Then the cosine of the angle between the unit vector to the Sun $\hat{x}_S$ and the vector along the symmetry axis is

$$\cos\theta_S = \hat{x}_S \cdot R_z(f')R_x(I)R_z(g'-f')R_x(J)\hat{z} . \quad (41)$$

Squaring this and expanding it as a Poisson series, we have the geometric part of the perturbation:

$$\cos^2\theta_S = \sum_{ijq} G_{ijq}(I, J)\cos(if' + jg' - q\lambda) . \quad (42)$$

The terms that involve both g' and λ are

$$G_{0,2,2}(I, J) = A_{0,2,2}(I)\sin^2 J , \quad (43)$$

$$G_{4,-2,2}(I, J) = A_{4,-2,2}(I)\sin^2 J , \quad (44)$$

$$G_{1,1,2}(I, J) = A_{1,1,2}(I)\sin J\cos J , \quad (45)$$

$$G_{3,-1,2}(I, J) = A_{3,-1,2}(I)\sin J\cos J , \quad (46)$$

where

$$A_{0,2,2}(I) = -\tfrac{1}{8}(1+\cos I)^2 , \quad (47)$$

$$A_{4,-2,2}(I) = -\tfrac{1}{8}(1-\cos I)^2 , \quad (48)$$

$$A_{1,1,2}(I) = -\tfrac{1}{2}(1+\cos I)\sin I , \quad (49)$$

$$A_{3,-1,2}(I) = +\tfrac{1}{2}(1-\cos I)\sin I . \quad (50)$$

There is a term that involves λ but not g':

$$G_{2,0,2}(I, J) = A_{2,0,2}(I)\left(1 - \frac{3}{2}\sin^2 J\right) \quad (51)$$

with

$$A_{2,0,2}(I) = -\tfrac{1}{2}\sin^2 I . \quad (52)$$

And there are terms that involve g' but not λ:

$$G_{1,-1,0}(I, J) = A_{1,-1,0}(I)\sin J\cos J ,$$
$$G_{2,-2,0}(I, J) = A_{2,-2,0}(I)\sin^2 J \quad (53)$$

with

$$A_{1,-1,0}(I) = \sin I\cos I , \quad A_{2,-2,0}(I) = \sin^2 I . \quad (54)$$

There are also terms that do not depend on the angles.

The orbital variables r and λ move nonuniformly; we expand the perturbation in terms of the mean anomaly M, longitude of perihelion ϖ, eccentricity e, and semimajor axis a. For any combination of angles ϕ and true anomaly l ($\lambda = \varpi + l$),

$$\left(\frac{a}{r}\right)^3 \cos(\phi - ql) = \sum_k X_k^q(e)\cos(\phi - kM) . \quad (55)$$

The coefficients $X_k^q(e)$ are special cases of the Hansen coefficients (see Plummer 1962). The Hansen coefficients can be written as a power series in eccentricity; the leading terms for $q = 2$ are $X_3^2(e) = 7e/2$, $X_2^2(e) = 1$, $X_1^2(e) = -e/2$, $X_0^2(e) = 0$, $X_{-1}^2(e) = -e^3/48$, and $X_{-2}^2(e) = -e^4/24$. The leading terms for $q = 0$ are $X_0^0 = 1$, $X_1^0 = X_{-1}^0 = 3e/2$, $X_2^0 = X_{-2}^0 = 9e^2/4$, $X_3^0 = X_{-3}^0 = 53e^3/16$, and $X_4^0 = X_{-4}^0 = 77e^4/16$.

We now identify the main resonances. We label the resonances by the tuple (i, j, q, k), where i, j, q, and k refer to the indices used in the sums above. The corresponding angular argument is $if' + jg' - kM - q\varpi$. The resonance amplitude involves the product $G_{ijq}(I, J)X_k^q(e)$. The amplitude factors are proportional to I^i and $e^{|k-q|}$ for small I and e. The angle f' moves slowly, with the period of the precession of the equinox, and the motion of longitude of perihelion ϖ is even slower, so the principal resonances occur for low-order commensurabilities between the tilt frequency and the orbital frequency. Resonances occur if $jg' - kM$ is slow. The angle g' moves opposite to the direction of rotation. For prograde rotation, g' regresses; for retrograde rotation, g' moves in the same direction as the orbital motion. The integer j has magnitude 1 or 2, so resonances occur if the core precession rate is a half-integral multiple of the orbital

frequency. Resonances that occur for prograde rotation (the spin and the orbital motion have the same sense) we term *prograde resonances*; those that occur for retrograde rotation we term *retrograde resonances.*

Most of the resonance terms depend on the angle f', so in principle, resonance passage can affect the obliquity. We expect, though, that this effect is small and defer further consideration of this possibility. Instead, we focus on the excitation of the core-mantle tilt mode. The obliquity, equinox, eccentricity, and perihelion are all slowly varying. For this analysis we assume that the obliquity and eccentricity are constant and the perihelion and equinox are prescribed linear functions of time. We assume the motion in the orbit is uniform: $M = nt$. The wobble mode is not resonant; we continue to assume that it has zero amplitude. With this assumption, $g' = -\theta$ and $G' = (c^2/D)\Theta \approx [\delta/(1-\delta)]\Theta$.

The astronomical forcing of a coupled core-mantle system has also been discussed in a Hamiltonian framework by Getino (1995b). In that work, the system is linearized and approximate analytic expressions for the nutations are derived. The theory is compared with that of Kinoshita (1977) and Kinoshita & Souchay (1990) for the rigid Earth. Getino & Ferrándiz (2000) discuss the forced linear problem in the presence of dissipation. Our focus is on the nonlinear dynamics of the resonances, with and without dissipation.

5. PROGRADE ANNUAL RESONANCES

The prograde annual resonances are $(1,-1,0,1)$, $(2,-2,0,2)$, $(3,-1,2,1)$, $(4,-2,2,2)$, $(0,2,2,-2)$, and $(1,1,2,-1)$. The strongest resonance is $(1,-1,0,1)$.

For small J, the approximate prograde annual resonance Hamiltonian is

$$\begin{aligned} H_R = {} & \omega_2\Theta + \tfrac{1}{2}k\Theta^2 \\ & + \epsilon_{1,-1,0,1}\sqrt{2\Theta}\cos(\theta - nt + \psi_{1,-1,0,1}) \\ & + \epsilon_{2,-2,0,2}\,2\Theta\cos(2\theta - 2nt + \psi_{2,-2,0,2}) \\ & + \epsilon_{3,-1,2,1}\sqrt{2\Theta}\cos(\theta - nt + \psi_{3,-1,2,1}) \\ & + \epsilon_{4,-2,2,2}\,2\Theta\cos(2\theta - 2nt + \psi_{4,-2,2,2}) \\ & + \epsilon_{0,2,2,-2}\,2\Theta\cos(2\theta - 2nt + \psi_{0,2,2,-2}) \\ & + \epsilon_{1,1,2,-1}\sqrt{2\Theta}\cos(\theta - nt + \psi_{1,1,2,-1})\,. \end{aligned} \tag{56}$$

The amplitudes are

$$\begin{aligned} \epsilon_{1,-1,0,1} &= \kappa\frac{3e}{2}\sin I\cos I\frac{1}{\sqrt{C\omega}}\sqrt{\frac{\delta}{1-\delta}}\,, \\ \epsilon_{2,-2,0,2} &= \kappa\frac{9e^2}{4}\sin^2 I\frac{1}{C\omega}\frac{\delta}{1-\delta}\,, \\ \epsilon_{3,-1,2,1} &= -\kappa\frac{e}{2}\sin^2\frac{I}{2}\sin I\frac{1}{\sqrt{C\omega}}\sqrt{\frac{\delta}{1-\delta}}\,, \\ \epsilon_{4,-2,2,2} &= -\kappa\frac{1}{2}\sin^4\frac{I}{2}\frac{1}{C\omega}\frac{\delta}{1-\delta}\,, \\ \epsilon_{0,2,2,-2} &= \kappa\frac{e^4}{48}\cos^4\frac{I}{2}\frac{1}{C\omega}\frac{\delta}{1-\delta}\,, \\ \epsilon_{1,1,2,-1} &= \kappa\frac{e^3}{48}\cos^2\frac{I}{2}\sin I\frac{1}{\sqrt{C\omega}}\sqrt{\frac{\delta}{1-\delta}} \end{aligned} \tag{57}$$

with

$$\kappa = \frac{3}{2}\frac{GmM_S R^2 J_2}{a^3} \approx \frac{3}{2}n^2 mR^2 J_2\,, \tag{58}$$

using the approximation $n^2 = GM_S/a^3$. The slow phases are

$$\begin{aligned} \psi_{1,-1,0,1} &= f'\,, \quad \psi_{2,-2,0,2} = 2f'\,, \\ \psi_{3,-1,2,1} &= 3f' - 2\varpi\,, \quad \psi_{4,-2,2,2} = 4f' - 2\varpi\,, \\ \psi_{0,2,2,-2} &= 2\varpi\,, \quad \psi_{1,1,2,-1} = -f' + 2\varpi\,. \end{aligned} \tag{59}$$

We have used the approximation for small J

$$\sin^2 J = 1 - \frac{L^2}{G^2} \approx \frac{2G'}{L'+N} \approx \frac{2G'}{C\omega}\,, \tag{60}$$

as before.

Performing a (time dependent) canonical transformation to $w = \theta - nt$ and $W = \Theta$, the new Hamiltonian is

$$\begin{aligned} H'_R = {} & (\omega_2 - n)W + \tfrac{1}{2}kW^2 \\ & + \epsilon_{1,-1,0,1}\sqrt{2W}\cos(w + \psi_{1,-1,0,1}) \\ & + \epsilon_{2,-2,0,2}\,2W\cos(2w + \psi_{2,-2,0,2}) \\ & + \epsilon_{3,-1,2,1}\sqrt{2W}\cos(w + \psi_{3,-1,2,1}) \\ & + \epsilon_{4,-2,2,2}\,2W\cos(2w + \psi_{4,-2,2,2}) \\ & + \epsilon_{0,2,2,-2}\,2W\cos(2w + \psi_{0,2,2,-2}) \\ & + \epsilon_{1,1,2,-1}\sqrt{2W}\cos(w + \psi_{1,1,2,-1})\,. \end{aligned} \tag{61}$$

There are three first-order resonances, $(1,-1,0,1)$, $(3,-1,2,1)$, and $(1,1,2,-1)$, and there are three second-order resonances, $(2,-2,0,2)$, $(4,-2,2,2)$, and $(0,2,2,-2)$.

Next we consider each resonance in turn as if it were isolated, ignoring the slow phases. First consider the first-order resonances. With $u = (2W)^{1/2}\cos w$ and $v = (2W)^{1/2}\sin w$, a first-order resonance Hamiltonian is of the form

$$H_1 = \Delta\left(\frac{u^2+v^2}{2}\right) + \frac{k}{2}\left(\frac{u^2+v^2}{2}\right)^2 + \epsilon u\,, \tag{62}$$

where $\Delta = \omega_2 - n$. The fixed points have $v = 0$ and satisfy

$$0 = \partial_u H_1 = (\omega_2 - n)u + \tfrac{1}{2}ku^3 + \epsilon\,. \tag{63}$$

Remember that k is negative. The amplitude ϵ can be either positive or negative. In the following discussion we will assume that ϵ is also negative; treating the positive-ϵ case is straightforward. If Δ is negative, then there is a single fixed point. If Δ is large and positive, then there are three fixed points, two stable and one unstable. The bifurcation occurs at

$$\Delta = (3/2)|\epsilon|^{2/3}|k|^{1/3}\,. \tag{64}$$

At the point of bifurcation, the stable/unstable pair form at

$$u_1 = (\epsilon/k)^{1/3} \tag{65}$$

and there is a stable fixed point at

$$u_2 = -2(\epsilon/k)^{1/3}\,. \tag{66}$$

At the point of bifurcation, the separatrix reaches $u = u_3 = 3u_2/2$. For a tidally evolving system that encounters this resonance in the direction for which capture does not occur, at the point of bifurcation there is a transient along the separatrix to $u = u_3$, followed by oscillations about the fixed point at $u = u_2$; with dissipation, the system settles on $u =$

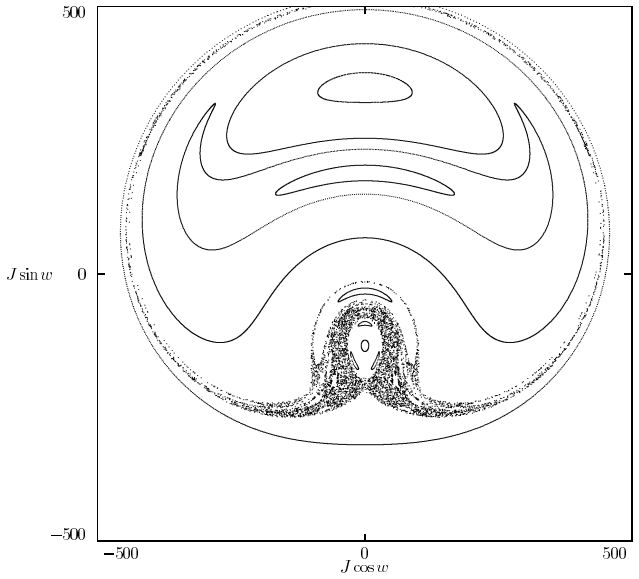

FIG. 1.—Surface of section for Earth near the prograde annual resonance, using a two-resonance model with fixed orbit and obliquity. The orbital eccentricity is 0.05, and the obliquity is 23°. The splitting frequency corresponds to an equinox precession period of 26,000 yr. The angle J is in arcseconds.

u_2. So u_2 sets the scale of the excitation during resonance passage. The corresponding angle J of offset of the symmetry axis from the total angular momentum is

$$\sin J \approx \frac{\sqrt{2G'}}{\sqrt{C\omega}} = 2\,\frac{1}{\sqrt{C\omega}}\left(\frac{\delta}{1-\delta}\right)^{1/2}\left(\frac{\epsilon}{k}\right)^{1/3} . \quad (67)$$

For small δ and I, this is approximately

$$\sin J_{ijql} \approx 2\delta\left(\frac{3}{2}\,\frac{n^2}{\omega^2}\,\frac{J_2}{f_c}\,\frac{mR^2}{C}\right)^{1/3}(A_{ijql})^{1/3} , \quad (68)$$

where J_{ijql} is the characteristic excitation for the resonance and A_{ijql} is the amplitude factor for the resonance.

Approximate values for Earth are $\delta = 0.11$, $J_2 = 0.001$, $C/MR^2 = 0.33$, and $f_c = 1/373$. At the annual resonance the rotation rate will be a bit larger than at present, and the obliquity will be a bit smaller. On long timescales both J_2 and f_c are proportional to ω^2, so the ratio remains constant. The characteristic scale of excitation of J for the $(1, -1, 0, 1)$ resonance is

$$J_{1,-1,0,1} \approx 339''\left(\frac{e}{0.05}\right)^{1/3}\left(\frac{I}{23^\circ}\right)^{1/3}\left(\frac{\omega_0}{\omega}\right)^{2/3} , \quad (69)$$

where ω_0 is the current rate of rotation of 2π radians per day. The transient along the separatrix is three-halves this, or about 508″, with the same parameter scaling. The characteristic scale of excitation for the $(3, -1, 2, 1)$ resonance is

$$J_{3,-1,2,1} \approx 82''\left(\frac{e}{0.05}\right)^{1/3}\left(\frac{I}{23^\circ}\right)\left(\frac{\omega_0}{\omega}\right)^{2/3} . \quad (70)$$

The characteristic scale of excitation for the $(1, 1, 2, -1)$ resonance is

$$J_{1,1,2,-1} \approx 11''\left(\frac{e}{0.05}\right)\left(\frac{I}{23^\circ}\right)^{1/3}\left(\frac{\omega_0}{\omega}\right)^{2/3} . \quad (71)$$

Ignoring the slow phases, the resonance Hamiltonian for the second-order resonances has the form

$$H_2 = \Delta\left(\frac{u^2+v^2}{2}\right) + \frac{k}{2}\left(\frac{u^2+v^2}{2}\right)^2 + \epsilon(u^2 - v^2) \quad (72)$$

with $\Delta = \omega_2 - n$. Recall that k is negative, ω_2 and n are positive. The sign of ϵ depends on the resonance; to simplify the discussion, we will assume that ϵ is negative. The fixed points occur on the coordinate axes. The fixed points for $u = 0$ satisfy

$$0 = \partial_v H_2 = (\Delta - 2\epsilon)v + \tfrac{1}{2}kv^3 . \quad (73)$$

So the fixed points are at $v = 0$ and $v^2 = -2(\Delta - 2\epsilon)/k$. As $k < 0$, the latter root is real for $\Delta > 2\epsilon$. The fixed points for $v = 0$ satisfy

$$0 = \partial_u H_2 = (\Delta + 2\epsilon)u + \tfrac{1}{2}ku^3 , \quad (74)$$

and the fixed points are at $u = 0$ and $u^2 = -2(\Delta + 2\epsilon)/k$. As $k < 0$, the latter root is real for $\Delta > -2\epsilon$. The two fixed points away from the origin with $u = 0$ are stable; the two fixed points away from the origin with $v = 0$ are unstable; the origin is stable except between the two bifurcations, where it is unstable. To give some scale to the strength of the resonance, we note that at the second bifurcation the stable fixed points have $v = v_2$ with $v_2^2 = -8\epsilon/k$. At this point the separatrix reaches $v = \sqrt{2}v_2$. The angle J of offset of the symmetry axis from the total angular momentum of the fixed point at the bifurcation is

$$\sin J \approx \frac{\sqrt{2G'}}{\sqrt{C\omega}} = \frac{1}{\sqrt{C\omega}}\left(\frac{\delta}{1-\delta}\right)^{1/2}\left(\frac{8\epsilon}{k}\right)^{1/2} . \quad (75)$$

For small δ and I, this is

$$\sin J_{ijql} \approx (2\delta)^{3/2}\left(\frac{3}{2}\,\frac{n^2}{\omega^2}\,\frac{J_2}{f_c}\,\frac{mR^2}{C}\right)^{1/2}(A_{ijql})^{1/2} . \quad (76)$$

The characteristic scale of excitation of J for the $(2, -2, 0, 2)$ resonance is

$$J_{2,-2,0,2} \approx 2''.5\left(\frac{e}{0.05}\right)\left(\frac{I}{23^\circ}\right)\left(\frac{\omega_0}{\omega}\right) . \quad (77)$$

The transient along the separatrix is $\sqrt{2}$ times this, or about 3″.5, with the same parameter scaling. The characteristic scale of excitation of J for the $(4, -2, 2, 2)$ resonance is

$$J_{4,-2,2,2} \approx 2''.4\left(\frac{I}{23^\circ}\right)^2\left(\frac{\omega_0}{\omega}\right) . \quad (78)$$

The characteristic scale of excitation of J for the $(0, 2, 2, -2)$ resonance is

$$J_{0,2,2,-2} \approx 0''.03\left(\frac{e}{0.05}\right)^2\left(\frac{\omega_0}{\omega}\right) . \quad (79)$$

We see that all the first-order resonances have a characteristic excitation that is larger than that of all the second-order resonances.

Having considered the resonances separately, we now consider them all together. The characteristic width (in frequency) of the largest resonance is the critical value Δ^* of $\Delta = \omega_2 - n$. But Δ^* is also the libration frequency at the point of bifurcation. The value of Δ^* is about 1.5×10^{-6} rad day^{-1}. To check for resonance overlap, we compare this width to the frequency separation of this largest resonance

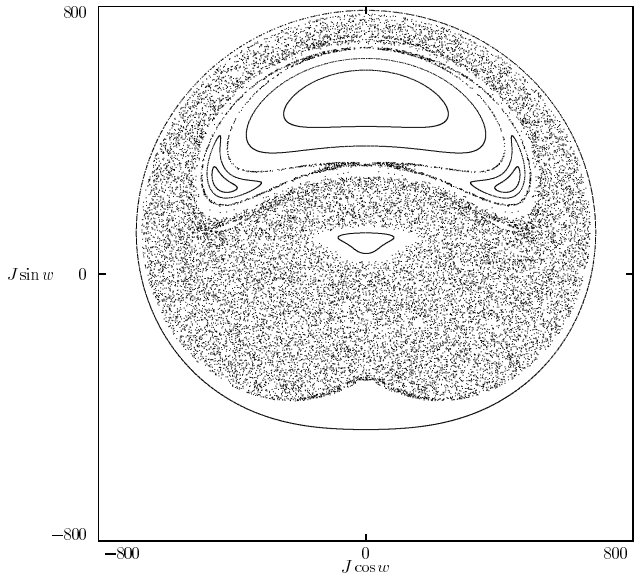

FIG. 2.—Surface of section for Venus near the retrograde annual resonance, for a simple model with the two largest resonances and constant splitting. The angle J is in arcseconds.

to the others. The splitting frequency is a multiple of the equinox precession frequency, which is about 6.6×10^{-7} rad day^{-1}. So there is indeed resonance overlap, and we should expect some chaotic behavior. However, the smaller resonances are too small to generate large-scale chaos. We can investigate this with surfaces of section for a simplified problem with only the two largest resonances, with constant obliquity and fixed orbit. On the surface of section (Fig. 1), near the point of bifurcation for the largest resonance we find a small chaotic zone near the unstable equilibrium, as expected.

6. OTHER PROGRADE RESONANCES

In general there are resonances when the core precession frequency is equal to any half-integral multiple of the orbital frequency, but the strongest prograde resonances occur at integral multiples.

There are six resonances with $\omega_2 \approx 2n$. The largest of these are the two first-order resonances $(3, -1, 2, 2)$ and $(1, -1, 0, 2)$. The characteristic excitation at the $(3, -1, 2, 2)$ resonance is

$$J_{3,-1,2,2} = 282''\left(\frac{I}{23^\circ}\right)\left(\frac{\omega_0}{\omega}\right)^{2/3} . \quad (80)$$

The characteristic excitation at the $(1, -1, 0, 2)$ resonance is

$$J_{1,-1,0,2} = 143''\left(\frac{I}{23^\circ}\right)^{1/3}\left(\frac{e}{0.05}\right)^{2/3}\left(\frac{\omega_0}{\omega}\right)^{2/3} . \quad (81)$$

These two resonances have strong resonance overlap, so we should expect a chaotic zone in the phase space.

There are also six resonances with $\omega_2 \approx 3n$. The largest of these is the first-order resonance $(3, -1, 2, 3)$. The characteristic excitation is

$$J_{3,-1,2,3} = 158''\left(\frac{I}{23^\circ}\right)\left(\frac{e}{0.05}\right)^{1/3}\left(\frac{\omega_0}{\omega}\right)^{2/3} . \quad (82)$$

7. RETROGRADE RESONANCES

We have in mind a speculative history of the rotation of Venus. Suppose that Venus was initially spinning much faster than it is today, but still retrograde. Today, Venus has near-zero obliquity as a consequence of tidal friction. We may suppose that it had nonzero obliquity in the past. As Venus was slowed by solar tidal friction, the system would pass through various retrograde core-mantle resonances. We consider here only the retrograde annual resonances.

There are six retrograde annual resonances. Of the three first-order resonances, the two largest, $(1, 1, 2, 1)$ and $(1, -1, 0, -1)$, are of comparable strength. The next strongest resonance, $(0, 2, 2, 2)$, is second order.

The characteristic scale of the excitation for the $(1, 1, 2, 1)$ resonance is

$$J_{1,1,2,1} = 330''\left(\frac{I}{23^\circ}\right)^{1/3}\left(\frac{e}{0.05}\right)^{1/3}\left(\frac{\omega_0}{\omega}\right)^{2/3} . \quad (83)$$

The characteristic scale of the excitation for the $(1, -1, 0, -1)$ resonance is

$$J_{1,-1,0,-1} = 469''\left(\frac{I}{23^\circ}\right)^{1/3}\left(\frac{e}{0.05}\right)^{1/3}\left(\frac{\omega_0}{\omega}\right)^{2/3} . \quad (84)$$

The characteristic scale of the excitation for the $(0, 2, 2, 2)$ resonance is

$$J_{0,2,2,2} = 92''(\omega_0/\omega)^{2/3} . \quad (85)$$

The excitation at the other resonances is smaller.

The annual retrograde resonances are strong and close. So we should find abundant chaos in the phase space. This is confirmed by looking at surfaces of section for the simplified problem with only the two largest resonances, with constant eccentricity 0.057 and obliquity 23°, and constant splitting frequency corresponding to a precession period for the equator of 22,800 yr. A sample section is shown in Figure 2. The chaotic zone for this hypothetical Venus near the retrograde annual resonance extends from 0″ to nearly 800″.

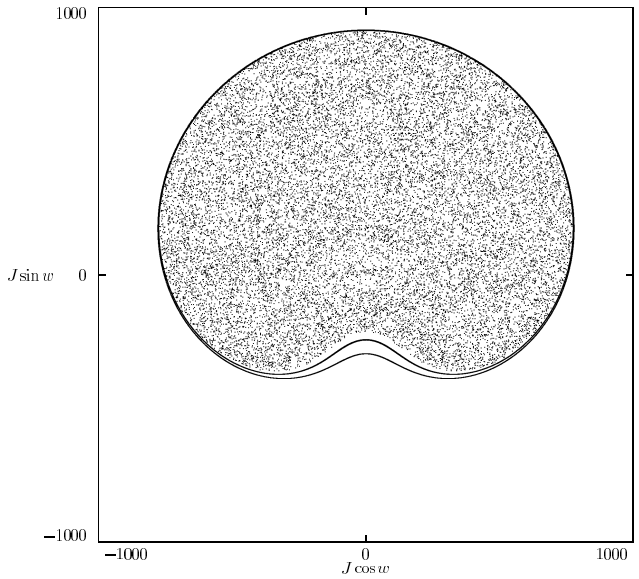

FIG. 3.—Same as Fig. 2, but for a model with a single resonance with periodically varying eccentricity.

Actually, the evolution of the system near the retrograde annual resonance is too complicated to be captured by the simple two-resonance model with constant eccentricity, obliquity, and splitting. The variation of the eccentricity also gives rise to chaotic behavior even for a single resonance, through the mechanism of adiabatic chaos (Wisdom 1985; Touma & Wisdom 1993). The separatrix of the single resonance with slowly varying strength pulsates, driving the system repeatedly across the separatrix. A representative surface of section for the retrograde annual resonance, including only the largest resonance term, but with periodically varying eccentricity, is shown in Figure 3. The whole oscillation region is engulfed by a chaotic zone, which reaches about 900″.

8. DISSIPATION

There are two dissipative processes to consider: dissipation that damps any core-mantle offset, and dissipation that changes the length of day.

That there will be dissipation of energy if the core is offset from the mantle is unquestioned. However, the dominant mechanism for this dissipation and its magnitude are uncertain. Toomre (1974) investigated viscous and magnetic coupling. Anelasticity of the mantle is also mentioned as a possibility. Recent VLBI results suggest that magnetic coupling is the dominant dissipative mechanism (Mathews et al. 1991).

Considering the uncertainty in core-mantle damping mechanisms, we adopt a simple dissipative law with quality factor Q. We assume that, if not subject to forcing, the energy in the core mode damps exponentially. Specifically, we assume

$$\frac{d\Theta}{dt} = -\frac{\omega_2}{Q}\,\Theta \tag{86}$$

and add corresponding terms to Hamilton's equations. In the geophysical literature, the core-mantle Q is sometimes defined with respect to the frequency of rotation rather than the frequency of core precession and, so, is larger than the Q used here by a factor ω/ω_2.

For dissipation in a laminar boundary layer with viscosity 0.01 $\mathrm{cm^2\ s^{-1}}$ and a rotation period of a day, the Q is estimated to be 12,000 (Toomre 1974). For a turbulent boundary layer or magnetic damping, the Q can be up to 2 orders of magnitude smaller (Mathews et al. 1991). Defraigne, Dehant, & Hinderer (1994) give an estimate of 75 ± 25 for the effective core Q of Earth.

Next we relate Q to the rate at which energy is dissipated if the core is offset from the mantle. The total energy of the core-mantle system with a nonzero tilt-mode amplitude and no wobble is

$$\begin{aligned} H_T &= \frac{1}{2\gamma}\,[C_c(L+N)^2 + CN^2 - 2C_c(L+N)N] + \omega_2\,\Theta \\ &= \frac{L^2}{C_m} + \frac{N^2}{C_c} + \omega_2\,\Theta\ . \end{aligned} \tag{87}$$

The last term in each expression is the energy in the tilt mode. The other terms are those neglected in deriving the linearized Hamiltonian; these neglected terms are approximately $C\omega^2/2$. Excitation of the tilt mode changes the angular momentum. The angular momentum with nonzero tilt-mode amplitude and no wobble is

$$\begin{aligned} G_T &= G' - S' + L' + N \\ &= L + N' + [\delta(1-2f_c) - 1]S' \\ &\approx C\omega[1 - \tfrac{1}{2}\delta(1-\delta)\,\sin^2 K]\ . \end{aligned} \tag{88}$$

Internal dissipation of tilt-mode energy conserves angular momentum, so the rotation rate ω' with zero tilt-mode amplitude satisfies

$$C\omega' = C\omega[1 - \tfrac{1}{2}\delta(1-\delta)\,\sin^2 K]\ . \tag{89}$$

The available energy is the difference between the system energy with nonzero tilt-mode amplitude and the system energy with zero tilt-mode amplitude and with the rotation rate adjusted to conserve angular momentum:

$$\begin{aligned} E &= \tfrac{1}{2}C\omega^2 + \omega_2\,\Theta - \tfrac{1}{2}C\omega'^2 \\ &\approx \tfrac{1}{2}(1-\delta)\delta C\omega^2\,\sin^2 K\ . \end{aligned} \tag{90}$$

Using equation (92), the rate of energy dissipation is approximately

$$\frac{dE}{dt} = \frac{1}{2}\,C\omega^2\delta(1-\delta)\,\frac{\omega_2}{Q}\,\sin^2 K \tag{91}$$

for small K. In terms of J, this is approximately

$$\frac{dE}{dt} = \frac{1}{2}\,C\omega^2\,\frac{1-\delta}{\delta}\,\frac{\omega_2}{Q}\,\sin^2 J\ . \tag{92}$$

Tidal friction from lunar and solar tides slows the rate of rotation of Earth. This changing rate of rotation serves to usher the system through various core-mantle resonances. Solar tides play a similar role for Venus. All the core-mantle resonances are encountered from the direction in which capture does not occur.

One might expect that the rate of rotation changes so slowly that the dynamics of resonance passage is unaffected by the finite rate of passage. It turns out, though, that this is only marginally the case. For the nonlinear resonance to significantly affect the evolution, the system must not pass through the resonance too quickly. Roughly, the time to pass through the resonance must be greater than the period of libration. As before, the characteristic resonance width (in frequency) is Δ^*, and the libration period at the point of bifurcation is $2\pi/\Delta^*$. So the first-order annual resonance is adiabatic if the rate of change of Δ is less than $\Delta^*/(2\pi/\Delta^*) = (\Delta^*)^2/2\pi$. This estimate was confirmed with numerical experiments.

For Earth, $\Delta^* \approx 1.5 \times 10^{-6}$ rad $\mathrm{day^{-1}}$. So to be in the adiabatic regime, the rate of change of Δ must be less than about 3×10^{-13} rad $\mathrm{day^{-1}}$ $\mathrm{day^{-1}}$. The actual rate is estimated to be about an order of magnitude smaller: 4×10^{-14} rad $\mathrm{day^{-1}}$ $\mathrm{day^{-1}}$. So, passage through the largest annual resonance is in the adiabatic regime. However, the weaker annual resonances, if taken by themselves, are not in the adiabatic regime. For Venus, the resonances are stronger and the rate of tidal evolution is slower, so evolution through the largest retrograde annual resonances, taken in isolation, is in the adiabatic regime.

Evolution must be much slower than the single-resonance adiabatic limit for a system to fully exhibit the range of chaotic behavior that is present in the Hamiltonian resonance models. For both Earth and Venus, the rate of

tidal evolution is large enough that the chaotic behavior of the Hamiltonian models is not fully exhibited in the evolution.

9. PROGRADE RESONANCE ENCOUNTER TIMES

To determine the times at which these core-mantle resonances were encountered, we must know the core precession frequency as a function of time. The core precession frequency depends on the core flattening, which depends on the rate of rotation of Earth. The rotation rate of Earth is modified by tidal friction.

Taking into account the elasticity of the mantle, the core precession frequency is approximately

$$\omega_2 = \omega(f_c - \beta)C/C_m\,, \tag{93}$$

where β is estimated to be $\beta = 0.00061$ for Earth (Mathews et al. 1991). This is to be compared with the core precession frequency without elasticity (eq. [31]). The hydrostatic core flattening scales with the square of the rotation rate, as does the elastic correction. So the hydrostatic core precession frequency scales simply as the cube of the rotation rate. The hydrostatic core precession period is about 460 days; the observed core precession period is about 430 days. We expect that the core precession frequency in the past is similarly given by the hydrostatic value plus some adjustment, say, 5%, due to nonhydrostatic flattening.

The annual resonance was reached when the rotation rate was $(460/365.25)^{1/3}$ faster than today, for hydrostatic flattening. For this rotation rate, the day is about 22.224 hr. Taking the observed deviation of the flattening from the hydrostatic flattening as typical, we might expect a 5% variation in precession frequency due to nonhydrostatic effects. This gives a range of length of day from 21.761 to 22.729 hr. Similarly, at the 2:1 resonance the rotation period is 17.639 hr. Allowing a 5% variation in flattening, we obtain a range of length of day from 17.272 to 18.040 hr. At the 3:1 resonance, we obtain a range of length of day from 15.088 to 15.760 hr.

The challenge is determining when the length of day of Earth was in these intervals. The rate of tidal evolution of the Earth-Moon system has surely not been constant, and it must be smaller in the past to prevent the Moon from being close to Earth too recently. Using the model of Touma & Wisdom (1994b, 1998), which is consistent with the rate of tidal evolution from lunar laser ranging (Dickey et al. 1994), the annual resonance occurs about 257 million years ago, for hydrostatic flattening, and between 183 and 323 million years ago, with as much as 5% nonhydrostatic flattening. Evidence from corals, bivalves, and tidal rhythmites suggests that the rate of tidal evolution has not changed substantially over the last 900 million years (Lambeck 1980; Sonett et al. 1996).

The suggestion has been made that passage through the annual resonance may be related to the major extinction and massive basalt flows at the Permo-Triassic boundary (e.g., Hinderer et al. 1987; Greff-Lefftz & Legros 1999). The Permo-Triassic boundary occurs about 251.4 ± 0.3 million years ago (Bowring et al. 1998). Alternatively, passage through the annual resonance has been associated with increased thermal activity 500–570 million years ago (Williams 1994); this timing is based on an alternate interpretation of tidal rhythmite data. Greff-Lefftz & Legros (1999) associate other core-mantle resonances (2:1 and 3:1) with periods of crustal formation (at 1.8 and 3.0 Gyr). They assume the rate of change of Earth's rotation is given by the piecewise linear model of Ross & Schubert (1989). In the Touma & Wisdom model, the 2:1 resonance occurs between 800 and 883 million years ago.

10. LINEAR EXCITATION

In this section, we derive the excitation and energy dissipation if the nonlinear terms are dropped from the equations of motion. We consider only the strongest annual resonances, which are first-order resonances.

Ignoring the nonlinear term and the slow phase, the resonance Hamiltonian is

$$H = \omega_2\,\Theta + \epsilon\sqrt{2\Theta}\,\cos\,(\theta - nt)\,. \tag{94}$$

Using canonical rectangular variables $x = (2\Theta)^{1/2}\cos\theta$ and $y = (2\Theta)^{1/2}\sin\theta$, this is

$$H = \omega_2\,\frac{x^2 + y^2}{2} + \epsilon(x\,\cos\,nt + y\,\sin\,nt)\,. \tag{95}$$

Hamilton's equations are

$$\frac{dx}{dt} = -\omega_2\,y - \epsilon\,\sin\,nt\,,\quad \frac{dy}{dt} = \omega_2\,x + \epsilon\,\cos\,nt\,. \tag{96}$$

Adding dissipation as described above,

$$\frac{dx}{dt} = -\frac{\omega_2}{2Q}\,x - \omega_2\,y - \epsilon\,\sin\,nt\,,$$

$$\frac{dy}{dt} = -\frac{\omega_2}{2Q}\,y + \omega_2\,x + \epsilon\,\cos\,nt\,. \tag{97}$$

In complex form with $\xi = x + iy$, the equations of motion are

$$\frac{d\xi}{dt} = -\frac{\omega_2}{2Q}\,\xi + i\omega_2\,\xi + i\epsilon\,\exp\,int\,. \tag{98}$$

The forced solution has a core offset angle of

$$\sin^2 J = \frac{\delta}{1-\delta}\,\frac{1}{C\omega}\left[\frac{\epsilon^2}{\Delta^2 + (\omega_2/2Q)^2}\right]. \tag{99}$$

Equation (99) for the linear excitation can be combined with equation (92) for the rate of energy dissipation to obtain the linear energy dissipation rate,

$$\frac{dE}{dt} = \frac{f_c\,\omega^2}{2Q}\,\frac{\epsilon^2}{\Delta^2 + (\omega_2/2Q)^2}\,. \tag{100}$$

At exact resonance ($\Delta = 0$), the peak linear excitation is

$$\sin^2 J = \frac{\delta}{1-\delta}\,\frac{1}{C\omega}\,\frac{4Q^2\epsilon^2}{\omega_2^2}\,. \tag{101}$$

The peak rate of energy dissipation is

$$\frac{dE}{dt} = \frac{2Q\epsilon^2}{f_c}\,. \tag{102}$$

The linear energy dissipation rate is proportional to Q at exact resonance.

To obtain an estimate of the total energy dissipated as the resonance is crossed, we can assume that Δ varies linearly with time with rate $\dot{\Delta}$. Approximating ω_2 by n at resonance

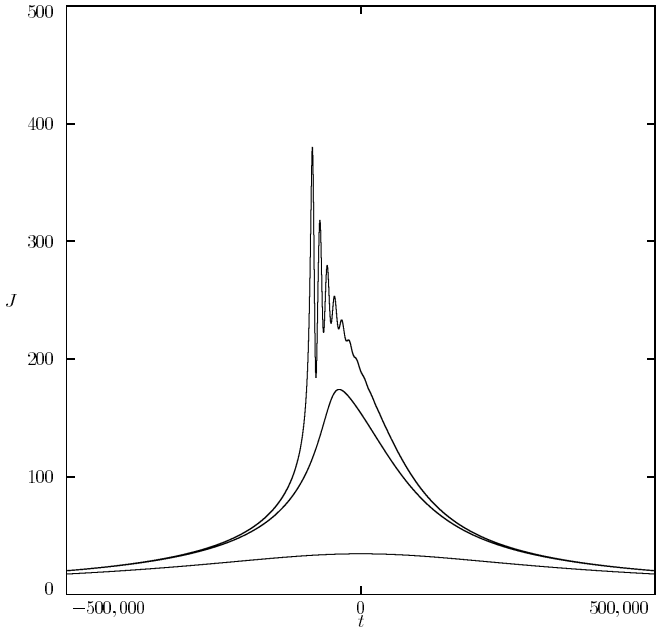

FIG. 4.—Core-mantle offset angle J (in arcseconds) vs. time (in years). The lower curve is for $Q = 2000$, the middle curve is for $Q = 10{,}000$, and the upper curve is for $Q = 50{,}000$.

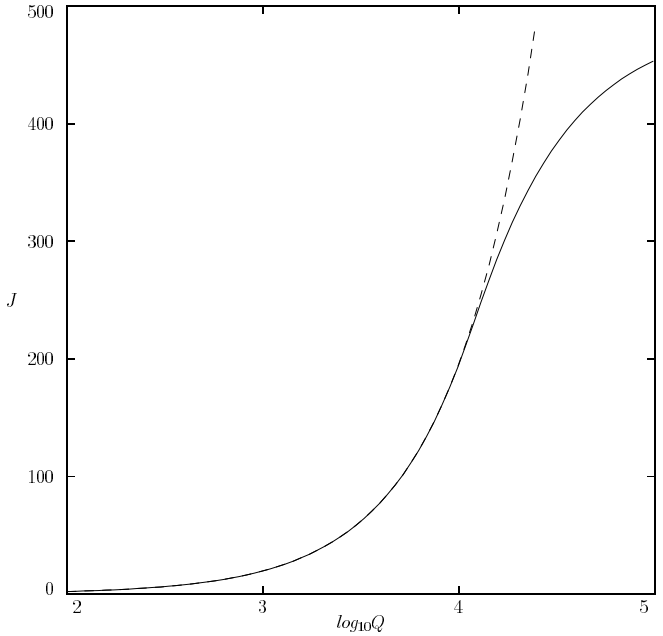

FIG. 6.—Peak excitation of the core-mantle offset (in arcseconds) vs. $\log Q$. The solid line is the nonlinear model; the dashed line is the linear model. Above about $Q = 10{,}000$ we begin to see the nonlinear saturation of the excitation.

and integrating across the resonance, the total energy dissipated in crossing the resonance is

$$\Delta E = \pi n \epsilon^2 / (f_c \dot{\Delta}) \, . \tag{103}$$

Note that the total energy dissipated as the resonance is crossed in this linearized system is independent of Q.

For the Earth prograde annual resonance, with obliquity 23°, and using $\dot{\Delta} = 4 \times 10^{-14}$ rad day^{-1} day^{-1}, we find

$$\Delta E = 1.7 \times 10^{26} (e/0.05)^2 \text{ J} \, . \tag{104}$$

Using a specific heat of 1200 J kg^{-1} K^{-1} and a density of 5000 kg m^{-3}, this energy input would raise the temperature of a 100 km thick shell near the core-mantle boundary by about 4 K. Greff-Lefftz & Legros (1999) find a total energy dissipation of 5×10^{25} J (for an unspecified eccentricity).

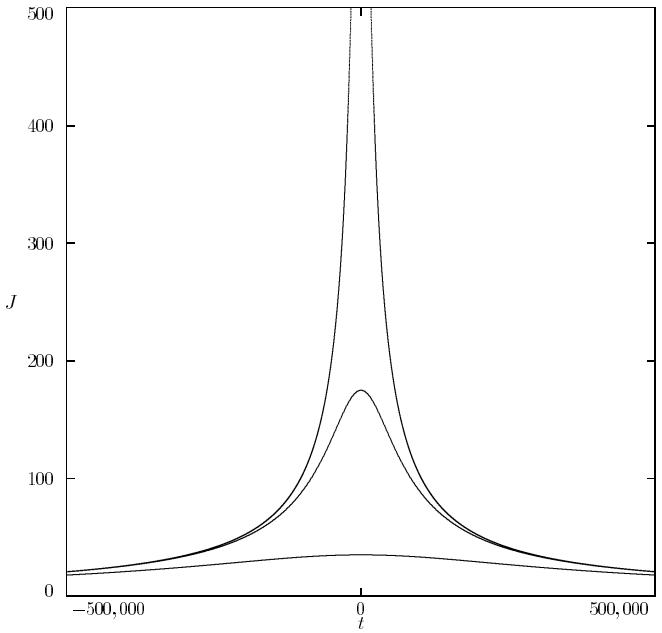

FIG. 5.—Linear estimate of the core-mantle offset angle J (in arcseconds) vs. time (in years). The lower curve is for $Q = 2000$, the middle curve is for $Q = 10{,}000$, and the upper curve is for $Q = 50{,}000$. The peak for $Q = 50{,}000$ is about 969″.

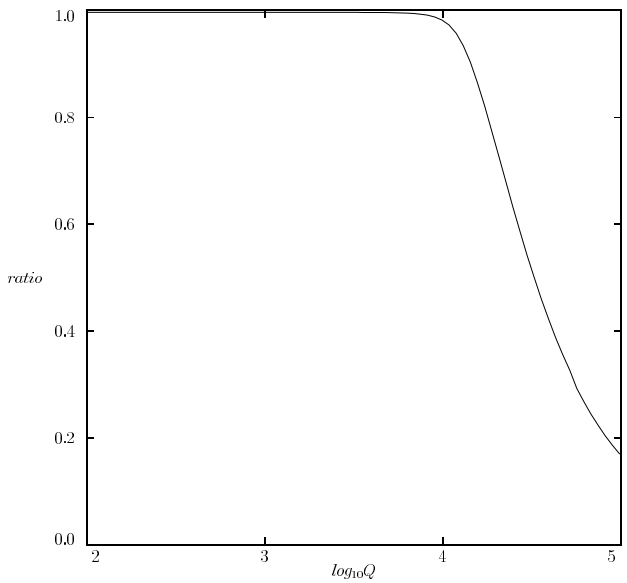

FIG. 7.—Ratio of the total energy dissipation to the linear estimate of the total energy dissipation vs. $\log Q$. Above about $Q = 10{,}000$, we begin to see how the nonlinear saturation of the excitation amplitude reduces the total energy input.

For the Venus retrograde annual resonance, with obliquity 23°, and using $\dot{\Delta} = 1 \times 10^{-14}$ rad day^{-1} day^{-1}, we find

$$\Delta E = 4.1 \times 10^{27}(e/0.05)^2 \text{ J} . \quad (105)$$

This is about 24 times larger than the energy dissipated in crossing the Earth annual resonance.

11. EVOLUTION THROUGH THE PROGRADE ANNUAL RESONANCE

The evolution of Earth through the annual resonance is shown in Figure 4. In this evolution we include the largest two terms in the resonance Hamiltonian (eq. [56]). We assume that the orbit is fixed, with an eccentricity of 0.05; we assume that the obliquity is constant at 23°, and that the equinox regresses uniformly with a period of 26,000 yr. We use the current rate of change of the rotation rate of Earth. We show the evolution for $Q = 2000$, $Q = 10{,}000$, and $Q = 50{,}000$.

The linear prediction for these three values of Q is shown in Figure 5. For $Q = 2000$, the linear and nonlinear models agree. For $Q = 10{,}000$, the peak excitations for the two models are similar, but the peaks are slightly shifted. For $Q = 50{,}000$, the two models yield substantially different evolutions. The peak excitation for the linear model is about 969″; the peak excitation for the nonlinear model is about 435″. Recall that the peak dissipation-free nonlinear excitation is 508″. The peak excitation of the core-mantle offset as a function of Q is shown in Figure 6. The energy dissipation as a function of Q is shown in Figure 7; the effect of nonlinear saturation is evident.

12. LIE-POISSON ALGORITHM FOR CORE-MANTLE COUPLING

We compare our analytic results and the results of our approximate resonance models with full numerical integrations of core-mantle Earth or Venus gravitationally coupled to the rest of the solar system. A free core-mantle system admits a Lie-Poisson structure, which is helpful in the construction of numerical algorithms that preserve the total angular momentum of the system. Such a structure was used in TW94a to construct a symplectic algorithm designed to evolve a rigid body coupled gravitationally to the Sun and planets. The Hamiltonian of the core-mantle system can be written in the form

$$H = H_{\rm CM} + H_{\rm Kepler} + H_{\rm coupling} , \quad (106)$$

where $H_{\rm CM}$ deals with free core-mantle dynamics in the Poincaré-Hough model, $H_{\rm Kepler}$ the Keplerian part of the orbital evolution, and $H_{\rm coupling}$ the gravitational interactions between the planets, as well as the spin-orbit coupling. The free rotational dynamics and the Keplerian motion commute, so once we know how to calculate the dynamics governed by $H_{\rm CM}$, it is trivial to couple it to the orbital motion with integrators of increasing order of accuracy, following the symplectic mapping algorithms of Wisdom & Holman (1991).

As already stated, the equations of motion for a Poincaré-Hough model of a fluid in a rotating shell can be written in a Lie-Poisson form. Given any Hamiltonian function H of $\boldsymbol{M}$ and $\boldsymbol{M}_c$, the corresponding vector field is

$$\frac{d\boldsymbol{M}}{dt} = \boldsymbol{M} \times \nabla_{\boldsymbol{M}} H, \quad \frac{d\boldsymbol{M}_c}{dt} = -\boldsymbol{M}_c \times \nabla_{\boldsymbol{M}_c} H . \quad (107)$$

These equations govern the evolution of $\boldsymbol{M}$ and $\boldsymbol{M}_c$ in the mantle frame. The evolution of that frame, represented by a special orthogonal transformation $C(t)$, is reconstructed as indicated in TW94a, by following an arbitrary fixed space vector $\boldsymbol{s}$ in the body frame, $\boldsymbol{s} = C(t)\boldsymbol{S}(t)$:

$$\frac{d\boldsymbol{S}}{dt} = \boldsymbol{S} \times \nabla_{\boldsymbol{M}} H . \quad (108)$$

Solving equation (108), we obtain $\boldsymbol{S}(t) = C^{-1}(t)C(0)\boldsymbol{S}(0)$, which yields $C^{-1}(t)$ and, thus, $C(t)$ by transposition (see TW94a for details).

We construct a Lie-Poisson algorithm, an algorithm that reduces the motion to a composition of elements of the Lie group on which the dynamics resides, by judicious splitting of the original Hamiltonian. For a triaxial body (the dynamics is in general not integrable), we did not succeed in constructing algorithms that used fewer than three sub-Hamiltonians. One such splitting involved

$$H_A = \frac{1}{2\alpha}(A_c P^2 + A P_c^2 - 2F_c P P_c) ,$$

$$H_B = \frac{1}{2\beta}(B_c Q^2 + B Q_c^2 - 2G_c Q Q_c) ,$$

$$H_C = \frac{1}{2\gamma}(C_c R^2 + C R_c^2 - 2H_c R R_c) . \quad (109)$$

These Hamiltonians generate rotations about the x, y, and z mantle axes. respectively. For instance, H_C leads to

$$\frac{d\boldsymbol{M}}{dt} = \boldsymbol{M} \times \boldsymbol{\Omega}_z^m , \quad \frac{d\boldsymbol{M}_c}{dt} = -\boldsymbol{M}_c \times \boldsymbol{\Omega}_z^c , \quad (110)$$

where $\boldsymbol{\Omega}_z^m = (0, 0, (C_c R - H_c R_c)/\gamma)$ and $\boldsymbol{\Omega}_z^c = (0, 0, (C R_c - H_c R)/\gamma)$. These equations preserve R and R_c and precess the vectors $\boldsymbol{M}$ and $\boldsymbol{M}_c$ about the z mantle axis with frequencies $w_z^m = (C_c R - H_c R_c)/\gamma$ and $w_z^c = (C R_c - H_c R)/\gamma$, respectively. Integrating equation (108), we find that $C(t) = C(0)C_z^{-1}(w_z^m t)$, where $C_z(\theta)$ rotates a vector about the z-axis by angle θ. Rotations about x, y, and z are then composed to yield symplectic algorithms of the desired order.

Our work is concerned with axisymmetric (oblate) bodies, for which the Poincaré-Hough model is integrable, and a splitting into two efficiently integrable sub-Hamiltonians is sufficient to reconstruct the dynamics. The Hamiltonian in this case reduces to

$$H_{\rm SCM} = \frac{1}{2\alpha}[A_c(P^2 + Q^2) + A(P_c^2 + Q_c^2) - 2F_c(P P_c + Q Q_c)] + \frac{1}{2\gamma}(C_c R^2 + C R_c^2 - 2H_c R R_c) . \quad (111)$$

We decompose it into

$$H_A = \frac{-F_c}{\alpha}(P P_c + Q Q_c + R R_c) ,$$

$$H_B = \frac{1}{2\alpha}[A_c(P^2 + Q^2) + A(P_c^2 + Q_c^2)] + \frac{1}{2\gamma}\left[C_c R^2 + C R_c^2 - 2\left(H_c - \frac{\gamma}{\alpha} F_c\right) R R_c\right] , \quad (112)$$

which, as we now demonstrate, are both integrable.

The Hamiltonian H_A yields

$$\frac{d\boldsymbol{M}}{dt} = -\boldsymbol{M} \times \frac{\boldsymbol{M}_c}{I}, \quad \frac{d\boldsymbol{M}_c}{dt} = \boldsymbol{M}_c \times \frac{\boldsymbol{M}}{I} \tag{113}$$

with $I = \alpha/F_c$. Note that these equations conserve $\boldsymbol{M}_d = \boldsymbol{M} - \boldsymbol{M}_c$ and can be rewritten as

$$\frac{d\boldsymbol{M}}{dt} = \boldsymbol{M} \times \frac{\boldsymbol{M}_d}{I}, \quad \frac{d\boldsymbol{M}_c}{dt} = \boldsymbol{M}_c \times \frac{\boldsymbol{M}_d}{I}. \tag{114}$$

Thus, both $\boldsymbol{M}$ and $\boldsymbol{M}_c$ precess about $\boldsymbol{M}_d$. The solution, $\boldsymbol{M}(t) = C_{\boldsymbol{\Omega}}(\sigma t)\boldsymbol{M}(0)$, $\boldsymbol{\Omega} = \boldsymbol{M}_d/I$, $\sigma = -|\boldsymbol{\Omega}|$, is given by the Euler-Rodrigues formula (see Goldstein 1980; TW94a). Next we solve for $\boldsymbol{S}(t)$:

$$\frac{d\boldsymbol{S}}{dt} = -\boldsymbol{S} \times \frac{\boldsymbol{M}_c(t)}{I}. \tag{115}$$

First transform to a frame precessing with $\boldsymbol{M}_c$, $\boldsymbol{S}(t) = C_{\boldsymbol{\Omega}}(\beta t)\boldsymbol{S}_p(t)$, to obtain

$$\frac{d\boldsymbol{S}_p}{dt} = \boldsymbol{S}_p \times \frac{\boldsymbol{M}(0)}{I}, \tag{116}$$

simply solved with the help of the Euler-Rodrigues formula: $\boldsymbol{S}_p(t) = C_{\boldsymbol{\Omega}_p}(\sigma_p t)\boldsymbol{S}_p(0)$, $\boldsymbol{\Omega}_p = \boldsymbol{M}(0)/I$, $\sigma_p = -|\boldsymbol{\Omega}_p|$. Finally, $S(t) = C_{\boldsymbol{\Omega}_p}(\sigma_p t)C_{\boldsymbol{\Omega}}(\sigma t)S(0)$. H_A is under control.

The Hamiltonian H_B is slightly more difficult to handle. The equations of motion

$$\frac{d\boldsymbol{M}}{dt} = \boldsymbol{M} \times \begin{pmatrix} (A_c/\alpha)P \\ (A_c/\alpha)Q \\ \dfrac{C_c}{\gamma} R + \left(\dfrac{F_1}{\alpha} - \dfrac{H_1}{\gamma}\right)R_c \end{pmatrix},$$

$$\frac{d\boldsymbol{M}_c}{dt} = \boldsymbol{M}_c \times \begin{pmatrix} (A/\alpha)P_c \\ (A/\alpha)Q_c \\ \dfrac{C}{\gamma} R_c + \left(\dfrac{F_1}{\alpha} - \dfrac{H_1}{\gamma}\right)R \end{pmatrix} \tag{117}$$

take the simpler form

$$\frac{d\boldsymbol{M}}{dt} = \boldsymbol{M} \times \begin{pmatrix} 0 \\ 0 \\ \Omega_z^m \end{pmatrix}, \quad \frac{d\boldsymbol{M}_c}{dt} = \boldsymbol{M}_c \times \begin{pmatrix} 0 \\ 0 \\ \Omega_z^c \end{pmatrix}, \tag{118}$$

where $\Omega_z^m = (C_c/\gamma - A_c/\alpha)R + (F_1/\alpha - H_1/\gamma)R_c$ and $\Omega_z^c = (C/\gamma - A/\alpha)R_c + (F_1/\alpha - H_1/\gamma)R$. These equations conserve both R and R_c and drive the rotation of both $\boldsymbol{M}$ and $\boldsymbol{M}_c$ about the mantle z-axis with frequencies Ω_z^m and Ω_z^c, respectively. We recover the evolution of the frame from

$$\frac{d\boldsymbol{S}}{dt} = \boldsymbol{S} \times \begin{pmatrix} (A_c/\alpha)P \\ (A_c/\alpha)Q \\ \dfrac{C_c}{\gamma} R + \left(\dfrac{F_1}{\alpha} - \dfrac{H_1}{\gamma}\right)R_c \end{pmatrix}, \tag{119}$$

which, when rewritten as

$$\frac{d\boldsymbol{S}}{dt} = \boldsymbol{S} \times \left[\frac{A_c}{\alpha}\boldsymbol{M} + \begin{pmatrix} 0 \\ 0 \\ \Omega_z^m \end{pmatrix}\right], \tag{120}$$

suggests the following treatment: Set $\boldsymbol{S}(t) = C_z(\Omega_z^m t)\boldsymbol{S}_p(t)$. Then

$$\frac{d\boldsymbol{S}_p}{dt} = \frac{A_c}{\alpha}\boldsymbol{S}_p \times C_z^{-1}\boldsymbol{M} - C_z^{-1}\frac{d}{dt}C_z\boldsymbol{S}_p + \boldsymbol{S}_p \times \begin{pmatrix} 0 \\ 0 \\ \Omega_z^m \end{pmatrix}. \tag{121}$$

The last two terms cancel, leaving

$$\frac{d\boldsymbol{S}_p}{dt} = \frac{A_c}{\alpha}\boldsymbol{S}_p \times \boldsymbol{M}(0). \tag{122}$$

So $\boldsymbol{S}_p$ precesses about $\boldsymbol{M}(0)$, and $\boldsymbol{S}(t)$ evolves by the composition of this precession with $C_z(\Omega_z^m t)$.

With these explicit solutions for the dynamics generated by both H_A and H_B, we construct a Lie-Poisson integrator for the free core-mantle body by interleaving the actions of H_A and H_B.

12.1. *Handling Dissipation*

The Hamiltonian dynamics is supplemented with two sources of dissipation. The first, tidal in origin, was treated in Touma & Wisdom (1994b), where the tidal evolution of the Earth-Moon system was studied. The second results from dissipative core-mantle interactions, which can be either magnetic or viscous in origin. The full dynamics is split into conservative and dissipative vector fields. The conservative field is calculated with the Lie-Poisson algorithm and is followed with a dissipative kick calculated with a first-order scheme, which for the applications being considered is sufficient.

Dissipation at the core-mantle interface results from fluid or magnetic stresses. Toomre (1966, 1974), among others, discusses both in detail. The upshot is that a torque is applied on the mantle, and an equal and opposite torque acts on the core, dissipating any velocity mismatch between fluid and mantle. Of course, the total angular momentum is not affected by such torques.

Independent of the form, how do such torques affect the core angular momentum variables that we use in the Lie-Poisson description? The mantle experiences a dissipative torque $\boldsymbol{T}_v$; its angular momentum $\boldsymbol{M}_m = \mathbf{I}_m\boldsymbol{w}$ changes: $d\boldsymbol{M}_m/dt = \boldsymbol{T}_v$. Here $\mathbf{I}_m = \mathbf{I} - \mathbf{I}_c$. This translates into a change of the mantle angular velocity, which by conservation of the total angular momentum affects the "angular velocity" of the fluid core $\boldsymbol{w}_c$:

$$\frac{d\boldsymbol{w}_c}{dt} = -\mathbf{I}_f^{-1}\,\mathbf{II}_m^{-1}\,\boldsymbol{T}_v. \tag{123}$$

Here $\mathbf{I}$, $\mathbf{I}_f$, and $\mathbf{I}_c$ are diagonal inertia tensors, with diagonals $\operatorname{diag}\mathbf{I} = (A, B, C)$, $\operatorname{diag}\mathbf{I}_f = (F_c, G_c, H_c)$, and $\operatorname{diag}\mathbf{I}_c = (A_c, B_c, C_c)$. Thus we obtain the rate of change of $\boldsymbol{M}_c$:

$$\frac{d\boldsymbol{M}_c}{dt} = (\mathbf{I}_f\,\mathbf{I}_m^{-1} - \mathbf{I}_c\,\mathbf{I}_f^{-1}\,\mathbf{II}_m^{-1})\boldsymbol{T}_v. \tag{124}$$

For a nearly spherical core, with a small contribution to the total inertia of the system, the right-hand side reduces to $-\boldsymbol{T}_v$.

The integrated dissipative torque on the mantle is proportional to the differential angular velocity of the fluid core and the rigid mantle: $\boldsymbol{T}_v = \kappa'(p_c, q_c, r_c)$. The specific form of κ' depends on the nature of dissipation being considered. To compare with the analytic results, we characterize the decay of the core tilt mode by a quality factor Q. We parameterize the dissipation by the effective laminar viscosity regardless of the actual mechanism of dissipation. For a laminar layer, with $\kappa' = C_c\omega_2/2Q$, Q is approximately

$$Q = \frac{0.382R_c\,\omega_2}{2\sqrt{\nu\omega}}, \tag{125}$$

where ν is the kinematic viscosity of the fluid, R_c is the core radius, ω is the angular velocity, and ω_2 is the frequency of the core mode (Greenspan 1990).

13. SIMULATION RESULTS

The numerical simulations are meant to provide a check on the analytic work and the simplified resonance models, but they also allow the dynamics to be explored in regimes that are difficult to handle analytically. For instance, in the resonance models we assume that the obliquity is constant, and that the z-component of the angular velocity of the core matches that of the mantle, a condition that can break down for low enough effective viscosity. These assumptions are relaxed in our algorithms, which in addition allow an examination of the dynamics of obliquity and wobble when the core-mantle system is gravitationally coupled to the rest of the solar system. Our full numerical model includes all the planets (evolving chaotically, of course), the Moon, and the coupled core-mantle system for Earth or Venus. Direct and cross lunar and solar tidal interactions for Earth, the Moon, and Venus are taken into account. The initial conditions were taken from the calculation of TW94a. The step size was near 1 hour. We found that with larger step sizes (Chandler) wobble is artificially excited.

These simulations played a crucial role in the development of our analytical models. There is no room to hide when Newton is standing there glaring at you. Comparisons of the analytical results with the numerical results uncovered early errors in our analytic development and clarified its essential ingredients. More importantly, the full simulations uncovered crucial aspects of the evolution that we did not anticipate. Namely, a significant portion of the energy that is dissipated from friction at the core-mantle boundary comes out of the energy of rotation of the planet, enhancing the rate of despinning of the planet over that expected from tidal friction alone. Consequently, the time spent in the resonance is shorter than was expected and the total energy dissipated during resonance passage is smaller than was expected.

We began our investigations with enhanced tidal friction. This reduces the computational demands and allows a check on the analytical developments. Our expectation was that the results could be scaled to the estimated actual rates of tidal evolution. More specifically, we expected that if we enhanced the rate of tidal evolution by a factor of, say, 10, and then stretched the time scale accordingly, then the plot of the evolution of the core-mantle offset would be invariant. This expectation was confirmed for tidal evolution enhancements in the range 10–1000. Unfortunately, the scaling breaks down for realistic rates of tidal evolution, as we document below.

First, consider the evolution of Earth through the prograde annual resonance. We have examined the consequences of Earth's passage through resonance for a variety of tidal evolution rates and dissipation rates at the core-mantle interface. In Figure 8, we show the core-mantle offset as a function of time for one representative case: $\nu = 0.01$ cm^2 s^{-1}, giving an estimated Q at time of resonance of $Q = 15{,}000$, with the rate of tidal evolution enhanced over the actual estimated rate by a factor of 10.

For comparison, the core-mantle offset in the evolution computed with a simple two-resonance model is displayed in Figure 9. The eccentricity is constant in this two-resonance model with a value of 0.04835. This is the eccentricity in the full model at the time of peak excitation. We see that the evolution of the two-resonance model is in pretty good agreement with the full simulation (Fig. 8). Away from resonance, some differences can be traced to the fact that Earth's orbital eccentricity varies with time because of planetary perturbations in the full simulation, whereas the eccentricity is fixed in this resonance model.

However, upon closer examination we see that the peak excitation is slightly higher and the shape of the peak is slightly broader than in the full simulation. It turns out that in the full simulation, there is an enhancement of the rate of change of the length of day over that from tidal evolution alone. Energy is dissipated at the core-mantle boundary, and much of this energy comes from the rotational kinetic energy. So dissipation of energy leads to an enhancement of the rate of deceleration of the rotation. We call this effect *rotation feedback*. As a consequence of rotation feedback, the system spends less time in a resonance than one would otherwise estimate, and so the total energy dissipated as a resonance is crossed is less, by as much as an order of magnitude, than one would estimate without considering this feedback. Rotation feedback is thus an important effect that must be taken into account in estimating the conse-

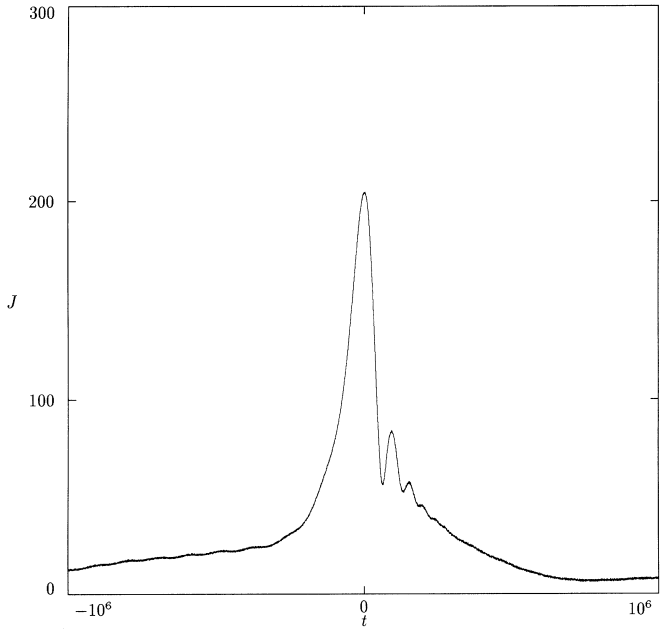

FIG. 8.—Core-mantle offset angle J (in arcseconds) vs. time (in years) for the full numerical simulation. The time origin has been chosen to coincide with the time of annual resonance passage. In this simulation the effective viscosity is $\nu = 0.01$ cm^2 s^{-1} and the rate of tidal evolution has been increased by a factor of 10 over the actual estimated rate.

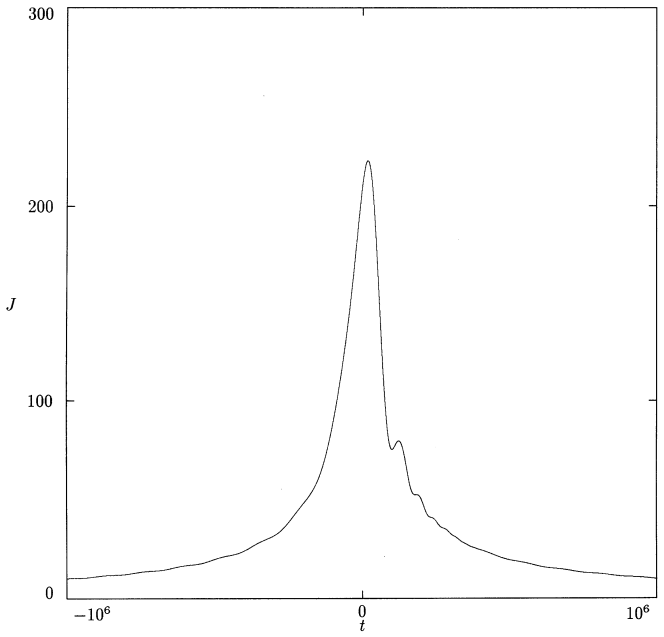

FIG. 9.—Core-mantle offset angle J (in arcseconds) vs. time (in years) for a two-resonance model. Here $\nu = 0.01$ cm^2 s^{-1} ($Q = 15{,}000$). The rate of tidal evolution has been increased by a factor of 10 over the estimated rate.

quences of core-mantle resonance passage. The full simulations were essential for uncovering this effect.

To include rotation feedback in the approximate resonance models, we need to estimate the additional deceleration of the rotation due to the dissipation of energy. As before, we work with an axisymmetric planet, in which a core-mantle friction (resulting from fluid viscosity, magnetic resistivity, or both) works to eliminate any relative velocity between the core and the mantle. Such relative velocities are excited by the passage through core-mantle resonance. For simplicity, and without serious loss of generality, we work with a dissipative torque of the form $\boldsymbol{T}_v = \kappa'(p_c, q_c, r_c)$. We are particularly interested in the z-component of the torque, which slows the rotation

$$\frac{d\omega}{dt} = \frac{\kappa'}{C_m} r_c \,, \tag{126}$$

where C_m is the mantle's moment of inertia about the axis of symmetry and r_c is nearly (for a spherical cavity this is exactly the case) the angular velocity of the core relative to the mantle. The rotation is also slowed by tidal friction.

We first express r_c in terms of the resonance dynamical action Θ. Recall that $r_c = (CR_c - C_cR)/\gamma$, or in terms of the Andoyer-like variables, $r_c = (CS - C_cL)/\gamma$. Following canonical transformation to the primed actions, $r_c = [(C - C_c)(N - S') - C_cL']/\gamma$. For the core tilt mode, with no wobble, $S' \approx \Theta/(1 - \delta)$. Recall that $\delta = C_c/C$. Note that $N + L' \approx Cr$ and $N \approx C_cr$, so as a consequence $CN - C_c(N + L) \approx 0$. Hence

$$r_c \approx -\frac{\Theta}{C_c(1 - \delta)} \,, \quad \frac{d\omega}{dt} \approx -\frac{\kappa'}{C_m C_c(1 - \delta)} \Theta \,. \tag{127}$$

Now,

$$\Theta \approx \tfrac{1}{2}(1 - \delta)\delta C\omega \sin^2 K \,, \tag{128}$$

so

$$\frac{d\omega}{dt} \approx -\frac{\kappa'}{2C_m} \omega \sin^2 K \,. \tag{129}$$

Recall that $\kappa' = C_c\omega_2/(2Q)$, and that the rate of energy dissipation $dE/dt \approx \frac{1}{2}C\omega^2\delta(1 - \delta)(\omega_2/Q)\sin^2 K$, so

$$\frac{d\omega}{dt} \approx -\frac{1}{2(1 - \delta)^2} \frac{1}{C\omega} \frac{dE}{dt} \,. \tag{130}$$

This expresses the additional rate of deceleration of the planet due to energy dissipation resulting from core-mantle tilt that is excited during resonance passage.

In Figure 10, we show the rate of change of the rotation from both the full simulation and a resonance model to which has been added the additional deceleration due to rotation feedback. The agreement is satisfactory.

Having clarified the main physical effects with artificially accelerated tidal friction, we now investigate the evolution of Earth through the annual resonance at a more realistic rate of tidal evolution. Figure 11 shows the core offset angle versus time without any enhancement of the rate of tidal evolution. Note how much sharper the peak is compared with the evolution with enhanced tidal evolution. Rotation feedback enhances the rate of change of the rate of rotation ($\dot{\omega}$) near the peak more than sixfold over tidal evolution alone. Here we have assumed that the orbit is fixed, with an eccentricity of 0.04835, that the obliquity is constant at 23°,

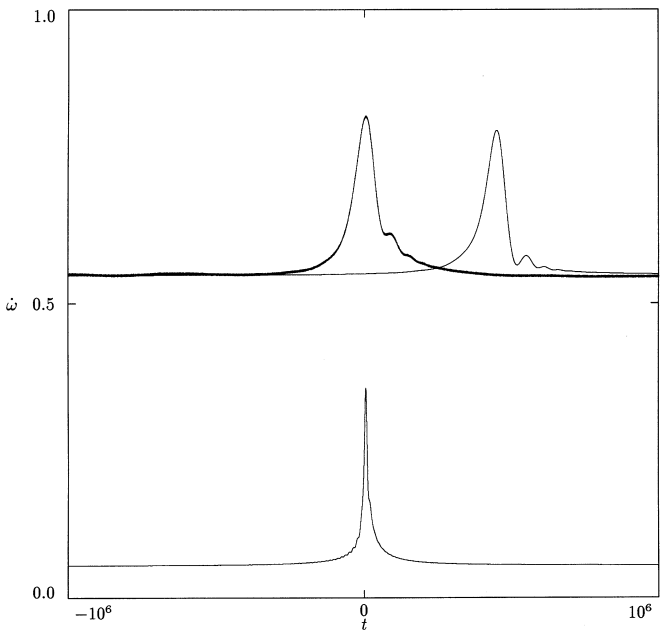

FIG. 10.—Rate of change of the rate of rotation ($\dot{\omega}$) vs. time. The rate of change of rotation is in 10^{-11} rad day^{-1} day^{-1}; the time is measured in years. The origin of time has no significance. For the upper two traces, the rate of tidal evolution is enhanced by a factor of 10. The trace with the peak in the center is from the full simulation. The trace with the peak displaced to the right is from the resonance model with rotation feedback. The rotation feedback resonance model is in satisfactory agreement with the full simulation. Rotation feedback enhances the rate of evolution by about 50%. In the upper two traces, the time scale is stretched to show the evolution as if there were no enhancement in the rate of tidal evolution. The lower trace is for the resonance model with rotation feedback without any enhancement of the rate of tidal evolution. At the resonance peak, rotation feedback enhances the rate of evolution by more than a factor of 6.

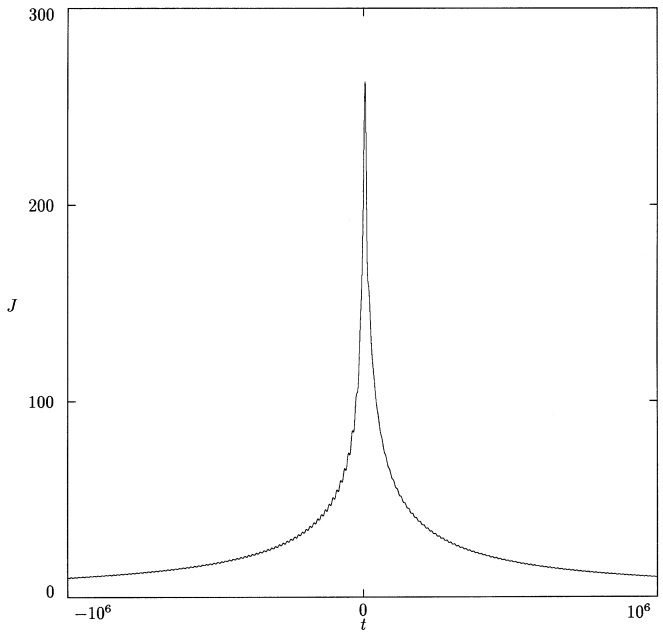

FIG. 11.—Core-mantle offset angle J (in arcseconds) vs. time (in years) for a two-resonance model with rotation feedback. Note how rotation feedback sharpens the peak. Here $\nu = 0.01$ cm^2 s^{-1} ($Q = 15{,}000$). The orbit is fixed with eccentricity 0.04835.

and that the equinox regresses uniformly with a period of 26,000 yr. The effective core viscosity is $\nu = 0.01$ cm^2 s^{-1} ($Q = 15{,}000$). For this case, we find that the total energy dissipated in passing through the prograde annual resonance, without rotation feedback, is about 1.82×10^{26} J, in good agreement with the linear estimates. Including rotation feedback reduces the total dissipated energy by about a factor of 3, to 6.32×10^{25} J.

Modeling the variation of Earth's orbit by the first four terms in the quasi-periodic series of Laskar (1988), we find the evolution of the core offset angle shown in Figure 12. The total dissipated energy is 3.74×10^{25} J. This value is sensitive to the eccentricity of Earth at the time of the core-mantle resonance encounter. These estimates are similar to that given by Greff-Lefftz & Legros (1999), who found 5×10^{25} J, for an unspecified eccentricity. They did not include rotation feedback.

We must also consider other values of the effective core Q. The rotation feedback effect is stronger at higher core offset because the rate of dissipation of energy is larger. At lower Q the excitations are lower, so rotation feedback is less effective at reducing the total energy dissipation. Figure 13 shows the total energy dissipated in Earth as a function of the effective Q. In these calculations the eccentricity of Earth is fixed at 0.05, and the obliquity is fixed at 23°. For Earth, the rotation feedback effect has a noticeable effect on the total energy deposited only if the effective core Q is larger than about 1000.

13.1. *Venus*

We looked at a hypothetical Venus, which starts out spinning retrograde with a rotation period of less than 19 hours. Its geophysical properties are Earth-like, except for the delay of the tidal bulge, which is taken to be a fifth of that on the present Earth. This value accounts for the fact that Venus has no oceans. The rate of tidal evolution for Venus is also different from that of Earth, because Venus has no moon and is closer to the Sun. The net effect is that the rate of tidal evolution ($\dot{\Delta}$) for Venus is estimated to be about a quarter that of Earth. As mentioned before, dissipation is parameterized by an effective viscosity in a laminar boundary layer. Other stresses will have a similar integrated form. Given the uncertainties about core viscosity, as well as mantle conductivity, we have explored a range of effective viscosity.

Figure 14 shows the excitation for Venus versus time for an effective viscosity of 10^{-4} cm^2 s^{-1} (a Q near resonance of

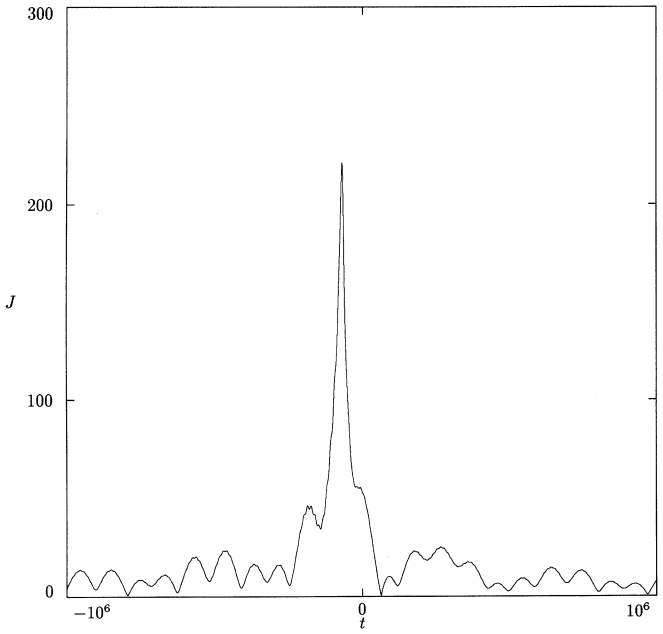

FIG. 12.—Core-mantle offset angle J (in arcseconds) vs. time (in years) for a two-resonance model with rotation feedback and Earth orbital variations. Here $\nu = 0.01$ cm^2 s^{-1} ($Q = 15{,}000$).

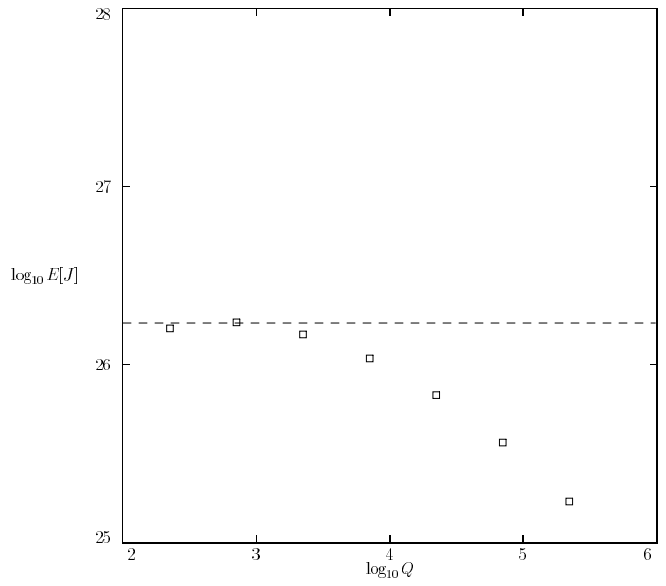

FIG. 13.—Energy dissipation in Earth vs. core-mantle Q, including rotation feedback. The obliquity is 23°; the orbital eccentricity is 0.05. The dashed line indicates the linear estimate, eq. (103), which is independent of Q. Rotation feedback is more important for larger Q.

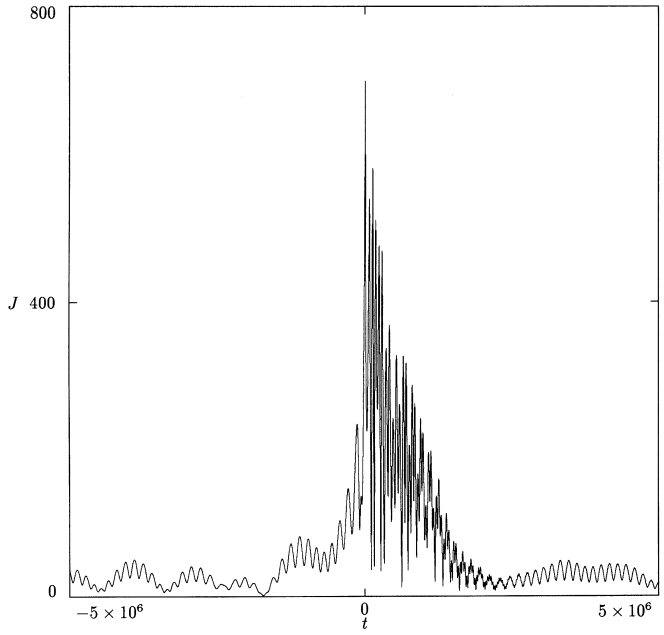

FIG. 14.—Amplitude of the core tilt mode (in arcseconds) for the full model vs. time (in years). Venus was started spinning with a period of 19 hr, an initial obliquity of 157° (retrograde rotation with obliquity 23°), and an equivalent core-mantle $Q = 2.26 \times 10^5$. The peak excitation of about 700″ reflects the extent of the chaotic zone in the inviscid limit. The rate of tidal evolution is enhanced by a factor of 10 relative to the estimated rate.

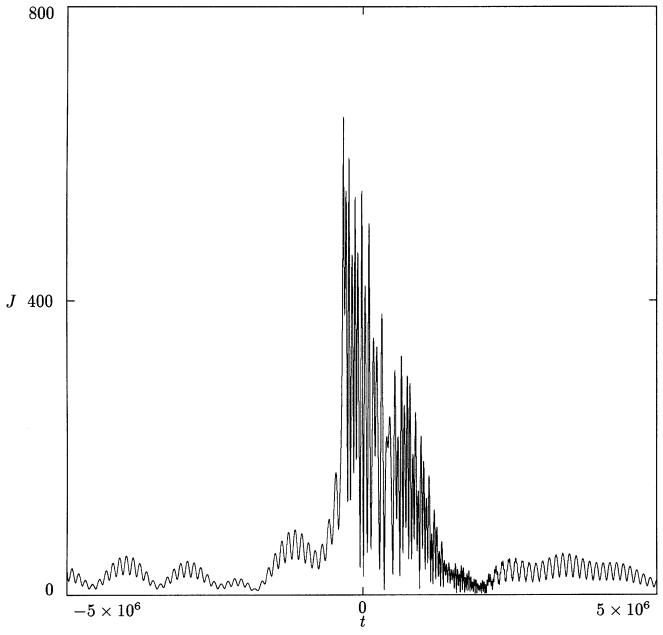

FIG. 15.—Amplitude (in arcseconds) of the core tilt mode vs. time (in years) for a two-resonance model with a quasi-periodic approximation to the orbital variations of Venus. This model includes rotation feedback. The equivalent core-mantle Q is 2.26×10^5. The obliquity is 23°, with retrograde rotation. The rate of tidal evolution is enhanced by a factor of 10 relative to the estimated rate, matching the rate of evolution in the full simulation.

226,000). The excitation reaches 700″, comparable to the maximum extent of the chaotic zone shown in Figure 2. The tidal evolution has been enhanced by a factor of 10 to reduce computational demands.

The excitation as a function of time for a two-resonance model with rotation feedback is shown in Figure 15. This model uses a four-term quasi-periodic model for the orbital variations of Venus (Laskar 1988). The two-resonance model and the full simulation are in satisfactory agreement.

Having achieved satisfactory agreement between the full simulation and the resonance model with accelerated tidal evolution, we can use the resonance model to explore the evolution of the system through the resonance at (estimated) realistic rates of tidal evolution. The evolution of the two-resonance model for the actual estimated rate of tidal evolution is shown in Figure 16. Even though the evolution is complicated and shows evidence of chaotic behavior, the actual energy dissipation (8.7×10^{25} J) is more than an order of magnitude smaller than the linear estimate. Rotation feedback substantially shortens the interval of large excitation. Also, nonlinear saturation is quite strong at such a high effective Q (see Fig. 7).

The total energy dissipated in Venus during passage through the retrograde annual resonance depends on several factors: the rate of tidal evolution, the effective core-mantle Q, and the obliquity at the time of passage. We may estimate the rate of tidal evolution using what is known about the tidal evolution of Earth's rotation as a guide. We have estimated that the rate of change of Δ for Venus is about a quarter that for Earth. Figure 17 shows the total energy deposited in Venus during passage through the annual resonance as a function of the enhancement factor, x, of the rate of tidal evolution relative to this nominal estimated rate. Roughly, the energy dissipation scales inversely with $\dot{\Delta}$, as in the linear estimate given in equation (103).

The total energy dissipated in Venus also depends on the effective core-mantle Q. Though the linear estimate is inde-

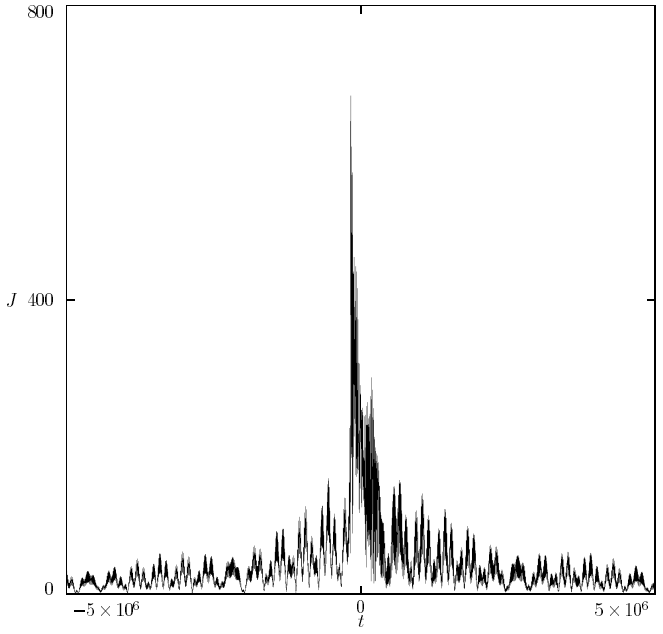

FIG. 16.—Amplitude (in arcseconds) of the core tilt mode vs. time (in years) for a two-resonance model with a quasi-periodic approximation to the orbital variations of Venus. The equivalent Q is 2.26×10^5. The rate of tidal evolution is the estimated rate, without any enhancement.

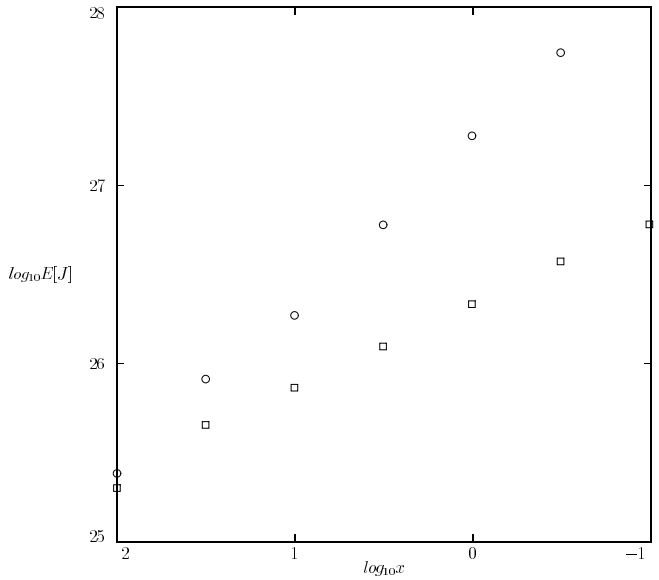

FIG. 17.—Energy dissipation in Venus vs. the logarithm of the tidal evolution enhancement factor, x, with (*squares*) and without (*circles*) rotation feedback. The obliquity is 23°. The effective core viscosity is 0.01 cm^2 s^{-1}.

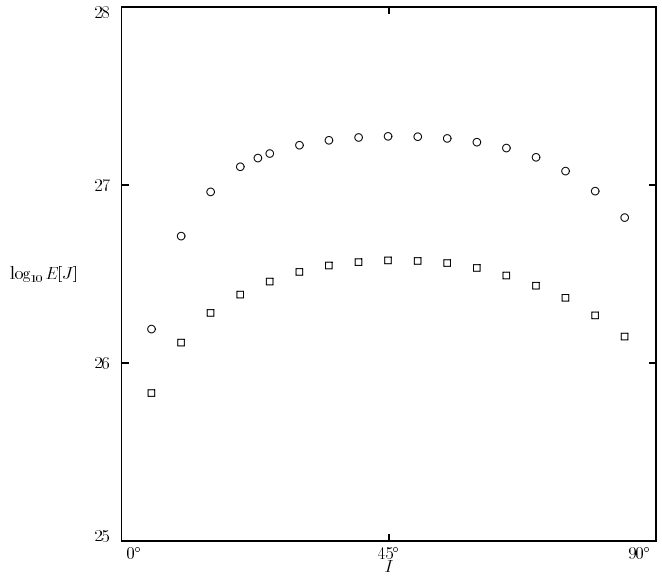

FIG. 19.—Total energy dissipation (joules) vs. obliquity (degrees), for effective core viscosity $\nu = 100$ cm^2 s^{-1} (*circles*) and $\nu = 0.01$ cm^2 s^{-1} (*squares*), with the two-resonance model with rotation feedback and quasi-periodic orbital variations.

pendent of Q, nonlinear saturation limits the amount of excitation and dissipation at large Q. The phenomenon of rotation feedback further reduces the amount of energy dissipation. Figure 18 shows the energy dissipation in Venus versus Q for a two-resonance model with rotation feedback and quasi-periodic orbital variations. The rotation is retrograde and the obliquity is 23°.

The strengths of the core-mantle resonances depend on the obliquity, but the obliquity that Venus might have had during the passage through the retrograde annual resonance is totally unconstrained. Figure 19 shows the total energy dissipation in Venus as a function of the obliquity at the time of resonance passage. The maximum energy dissipation occurs for an obliquity near 45°, but is within a factor of 2 of the maximum for any obliquity from about 15° to 75°.

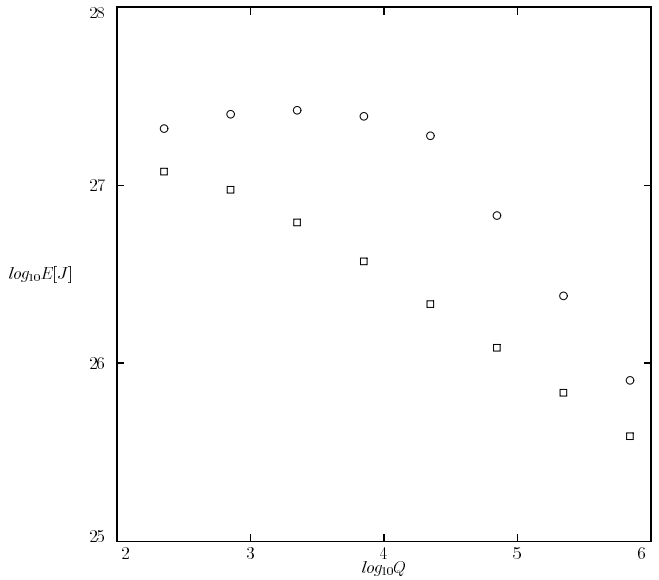

FIG. 18.—Energy dissipation (joules) in Venus vs. core-mantle Q, with (*squares*) and without (*circles*) rotation feedback. The obliquity is 23°.

14. SPECULATIONS CONCERNING VENUS

Traditionally, the spins of the planets have been thought to have been established by an orderly accretion process, a thought inspired by the fact that prograde rotations predominate in the solar system. Within this mind-set, the retrograde rotation of Venus is a puzzle framed by the question, "How did Venus flip over?" To this day, the discussion of the history of the rotation and obliquity of Venus focuses on initial prograde rotation states and possible mechanisms of turning Venus upside down (e.g., Goldreich & Peale 1970; Yoder 1995a; Néron de Surgy & Laskar 1997).

Recently, though, opinion has shifted to the idea that late, large impacts play a dominant role in establishing the spins of the terrestrial planets (Hartmann & Vail 1986; Lissauer & Safronov 1991; Dones & Tremaine 1993; Lissauer 1995). The spin that results from numerous large impacts may be either prograde or retrograde. In this view, a sequence of terrestrial planets with their spins all lined up (all prograde or all retrograde) would be a surprise. Think about tossing four coins. The most likely outcome is that three of the coins will be the same and one different (probability $\frac{1}{2}$). It is very unlikely that all will be the same (probability $\frac{1}{8}$). Among the terrestrial planets, three are prograde and one is retrograde. From this point of view, an initial retrograde rotation of Venus is not surprising. Indeed, why bend over backward to make Venus flip upside down? The simplest scenario for Venus is that the rotation has always been retrograde.

The rotation period of Mars (25 hr) is essentially primordial. When the Moon was close to Earth, the rotation period of Earth was near 5 hours. The initial rotation

period of Mercury is unknown. We might expect that the initial rotation period of the other terrestrial planets might be comparable to that of Mars and Earth. An initial retrograde rotation of Venus with a period shorter than 19 hours is plausible. If the initial rotation of Venus was retrograde and Venus initially had a rotation period shorter than about 19 hours, then Venus would have passed through the retrograde annual core-mantle resonance. (We are assuming an Earth-sized fluid core.)

We have estimated the energy deposited in Venus as the retrograde annual resonance was crossed (see § 13 for a detailed discussion of results). For the nominal rate of tidal evolution, the total energy deposited can be as large as 2×10^{27} J, for an effective core-mantle Q of order 100 (effective $\nu = 100$ cm^2 s^{-1}). For larger Q, the total energy deposited is smaller. For slower rates of tidal evolution, the energy that is deposited is larger. We may compare this with estimates of the energy deposited during passage of Earth through the prograde annual resonance, which occurred near the Permo-Triassic boundary 250 million years ago. The value depends on the eccentricity at the time of resonance passage; the energy deposited is of order 4×10^{25} J, with perhaps a factor of 2 uncertainty. Thus, the energy deposited in Venus in crossing the retrograde annual resonance could be nearly 50 times larger than the energy deposited in Earth during the prograde annual resonance passage.

It has been suggested that the Siberian traps, which occur at the Permo-Triassic boundary, and possibly even the Permo-Triassic extinction are a result of this resonance passage and the mantle plumes set in motion by this heat pulse. Further study is required to decide what role Earth's passage through the annual resonance had in the formation of the Siberian traps and the Permo-Triassic extinction. The timing is certainly suggestive, but it may just be a coincidence. On the other hand, if the Siberian traps are a result of passage through the annual core-mantle resonance, then we may speculate as to the consequences of as much as 50 times as much heating in Venus as the retrograde annual resonance was crossed. It seems a natural explanation of the global resurfacing of Venus. Venus has (and perhaps always has had) a retrograde rotation, and the rate of tidal evolution of the rotation of Venus is slower than for Earth. As a result, Venus is subjected to dramatically more resonant heating than Earth. Venus has been globally resurfaced, and Earth has the Siberian traps.

That is all very exciting, but there are serious problems. One issue is whether the energy that is deposited is sufficient to cause the global resurfacing of Venus (or the Siberian traps). Preliminary mantle convection simulations of this process have yielded promising results (B. Hager 2001, private communication). In a simulation in which 2×10^{27} J were deposited at the base of the mantle, sufficient heat was carried to the surface to generate 250 m global equivalent melt. It has been estimated that 500 m global equivalent melt was required to resurface Venus (Solomon, Bullock, & Grinspoon 1999). This is very encouraging, but further study is required.

The most serious problem is how to get from there to here. The core-mantle resonance occurs for a rotation period near 19.3 hr, but Venus rotates slowly today. Can tidal friction slow Venus from a rotation period of 19 hours to its current period of 243 days in less than a billion years (an estimated upper limit to the age of the surface of Venus)? For Venus to slow to its present rotation rate from a 19.3 hr rotation period in less than 1 Gyr requires an effective tidal Q less than 10, in the range 5–8. For comparison, the effective tidal Q of Mars is about 85, the tidal Q for the Moon is about 27, and the effective Q for Earth is about 12 (Yoder 1995b). The Q for Earth is dominated by ocean dissipation in the shallow seas. The Q of the Moon is thought to result from turbulent dissipation at a core-mantle boundary or to a partially molten layer in the mantle. Could the sort of heating that passage through the core-mantle annual resonance implies change the interior of Venus so that the time-average effective tidal Q is less than 10?

An interesting possibility is that there is especially large tidal dissipation in the several hundred meter deep magma ocean that is required to resurface Venus. The viscosity of molten rock is several orders of magnitude larger than the viscosity of water, so if Earth's oceans reduce the effective Q of Earth to 12, perhaps the effective Q of Venus would be much lower. Water and sulfur dioxide introduced into the atmosphere during resurfacing raise the temperature of the atmosphere (Solomon et al. 1999), slowing the cooling. Tidal dissipation (heating) might then act to maintain the magma ocean in a molten state while slowing rotation. In addition to supplying the melt for resurfacing the mantle, plumes might also create a partially molten or low-viscosity layer below the surface of Venus that might also reduce the effective tidal Q. These processes will be explored in another paper.

Another possibility that should be considered is that nonhydrostatic contributions to the flattening of the core-mantle boundary could actually drive the system back through any of these resonances. Core-mantle resonance passage might not be a one-time affair. Reverse passage through these resonances is significantly different from passage in the direction we have been considering. Two distinct mechanisms allow the system to be captured into resonance during reverse passage.

First, the nonlinear dynamics of first-order resonances allows capture for reverse passage. Indeed, for isolated first-order core-mantle resonances with constant obliquity and eccentricity, capture is certain for small initial core offsets if the rate of resonance passage (rate of change of nonhydrostatic flattening) is small enough. The actual outcome of resonance passage is more complicated to determine, because of the presence of dissipation, multiple resonances, and orbital variations. We have verified that reverse capture in these nonlinear first-order core-mantle resonances is possible through simulations with our resonance models. We defer further discussion to a future paper.

Rotation feedback provides another mechanism for resonance capture. An increase in the core flattening due to nonhydrostatic contributions can drive the system back toward the resonance. As the resonance is approached, the excitation increases and energy dissipation increases. But because of rotation feedback, as energy is dissipated there is an additional slowing of the rotation, which tends to make the system move away from resonance. An equilibrium is possible. As nonhydrostatic ellipticity changes drive the system back to resonance, rotation feedback drives the system away from resonance. The two effects can balance. What happens in this captured state is that the core precession frequency is maintained near resonance with the orbital mean motion. The way this happens is that the rotation rate

decreases to compensate for the increase in core ellipticity—the core precession frequency is proportional to the product of the ellipticity and the rotation rate. Of course, energy is dissipated as long as the system stays in resonance.

This raises another interesting possibility for slowing Venus down after resonance passage (and resurfacing). If the pattern of mantle convection that is responsible for the increase in the nonhydrostatic flattening is intensified by the heating generated by the resonance excitation, then a feedback is possible whereby the nonhydrostatic flattening monotonically grows, while rotation feedback constantly reduces the rotation rate, keeping the system in resonance and powering the further growth of nonhydrostatic flattening. The rotation rate could be substantially reduced by this process. If, say, the nonhydrostatic flattening contribution is so large as to double the total flattening, then the rotation rate will be reduced roughly by half (the hydrostatic contribution to the flattening is reduced as the rotation rate decreases). This could be a significant step in the process of slowing Venus. The process is only limited by how much nonhydrostatic flattening can be supported.

We have verified that this equilibrium exists by running the resonance models with additional nonhydrostatic contributions to the flattening and mapped out the parameters for which capture occurs. Essentially, the rate of increase of nonhydrostatic flattening must be large enough so that the resonance is encountered in the reverse direction, overcoming the decrease in hydrostatic flattening that occurs because of tidal slowing of the rotation. But we also find that if the rate of increase of nonhydrostatic flattening is too large, the system is not captured. We will report on these results in a future paper.

Even if it turns out that passage through the annual resonance is not directly related to the global resurfacing event, it is still possible that Venus passed through the annual resonance early in its history. The heating then may have dramatically altered the state of the atmosphere and interior and still be a part of the explanation of the divergent histories of Earth and Venus.

15. SUMMARY

This paper documents our extended investigations of the nonlinear dynamics of the astronomically forced coupled core-mantle system, which we began in 1993. To some extent this paper is a diary of our developing understanding of this problem. The astronomically forced core-mantle system is a beautiful problem that has never before been considered from a modern nonlinear dynamics point of view. We were drawn to it by its intrinsic interest and the fact that it offered fertile new unexplored territory for the application of modern methods of nonlinear dynamics. But also we began our investigation with the hunch (or hope) that core-mantle dynamics might play a role in the both the Permo-Triassic extinction and the resurfacing of Venus.

We have given an exact Hamiltonian formulation of the Poincaré-Hough model. We have given a novel Hamiltonian derivation of the normal modes of the linearized system. We have derived an approximate Hamiltonian governing the evolution of the tilt mode that includes the first nonlinear contribution. We then developed, in this Hamiltonian formulation, expressions for the perturbations. We have identified and derived the main resonance contributions near the principal core-mantle precession resonances. These are the resonances in which the period of precession of the core vorticity is commensurate with orbital period of the planet. For the most important resonances the core frequency is an integer multiple of the orbital mean motion, but there are also resonances that are half-integral multiples. We give analytic estimates of the excitation that would be expected at each resonance, if it were isolated. We focus attention on the prograde and retrograde annual resonances. We find that near each commensurability, there are actually multiple resonances with small frequency splitting due to the precession of the equinox and perihelion. The multiple overlapping resonances give rise to chaotic behavior. For Earth, with prograde rotation, the chaotic zones are small; for Venus, with retrograde rotation, the chaotic zones are large. The precession of the core is in the opposite direction to the rotation. For Venus, the core precesses in the same direction as Venus goes around the Sun, with great effect.

There are two distinct dissipative effects to consider. The rotation of the planet is slowed by tidal friction, and any core-mantle offset results in energy dissipation at the core-mantle boundary. We specify the magnitude of this dissipation by the effective Q but otherwise make no commitment to a specific dissipation mechanism. We estimate the times at which Earth passed through these core-mantle resonances. The annual resonance nominally occurs 257 million years ago, just before the Permo-Triassic extinction and the Siberian traps. The timing is suggestive but may, in the end, just be coincidence. As a point of comparison for our investigations of the nonlinear dynamics of resonance, we linearized our model and considered the excitation and energy dissipation in the linear regime. We find in the linear model that about 24 times as much energy is dissipated in Venus compared with Earth as each passes through the annual resonance. Turning to the nonlinear dynamics of resonance passage with dissipation, we find that for small Q the excitations are small and the evolution of the system is pretty well described by the linear model. As Q is increased the nonlinear dynamics becomes more important, and the fact becomes apparent that in the inviscid limit a separatrix is crossed as the resonance is encountered. For Q above about 10,000, the dynamical nonlinearity limits the magnitude of the excitation (nonlinear saturation) and limits the total energy dissipation.

We have developed new symplectic algorithms to study the evolution of the core-mantle system numerically. Our full numerical model describes a coupled core-mantle system, subject to astronomical perturbations from the full chaotically evolving solar system. The model includes direct and cross tidal friction on Earth and the Moon. The full simulations are compared with approximate resonance models. The approximate models are used to explore the parameter space; the full simulations provide a check on the approximate resonance models. Comparison of the two uncovered an important feedback effect: energy that is dissipated as a result of core-mantle offset comes primarily from the rotation, enhancing the rate of change of rotation over the rate expected from tidal evolution alone. A consequence is that the system spends less time in resonance than one would otherwise expect, and the total energy deposited is also reduced. We call this effect *rotation feedback*. Depending on the parameters under investigation, rotation feedback can reduce the total energy deposited by an order of magnitude. With rotation feedback included in the reso-

nance models, we mapped out the total energy dissipated in Earth and Venus, as a function of the various unknown parameters. Generally, for small effective core Q the total dissipation in Venus is as much as 20–50 times larger than the total dissipation in Earth.

This scenario for resurfacing Venus has many attractive features. The main difference that has resulted in such radically different present conditions on Earth and Venus might be as simple as the accident that Venus rotates in a retrograde sense and Earth in a prograde sense. Where does all the energy come from that is required to resurface Venus? Could it really come just from a rearrangement of the heat already in the interior? In our scenario, the energy that is required to resurface the planet is drawn from the kinetic energy of rotation of the planet. Though not infinite, the rotational kinetic energy is a very large reservoir (about 2.5×10^{29} J). There is plenty of available energy. The energy that is dissipated during resonance passage (as much as 2×10^{27} J) seems to be sufficient to initiate the resurfacing of Venus. Preliminary mantle convection simulations (B. Hager 2001, private communication) have produced encouraging results concerning resurfacing, given the amount of resonant heating we have estimated here. Venus must slow down to the present slow rate of rotation in the billion or so years since resurfacing. A number of possible braking mechanisms were presented. Further study is required.

This research was supported in part by the NASA Planetary Geology and Geophysics Program. We thank Sam Bowring, Tim Grove, Brad Hager, Tom Herring, Bill McKinnon, S. Sridhar, Sean Solomon, Gerald J. Sussman, Ori Weisberg, Kevin Zahnle, and Maria Zuber for helpful discussions. We are grateful to an anonymous reviewer for helpful suggestions and for pointing out the interesting work of Getino & Ferrándiz. We thank the staff of the Specola Vaticana for their hospitality while this work was being completed.

REFERENCES

Andoyer, H. 1923, Cours de mechanique celeste, Vol. 1 (Paris: Gauthier-Villars)
Bowring, S. A., Erwin, D. H., Jin, Y. G., Martin, M. W., Davidek, K., & Wang, W. 1998, Science, 280, 1039
Defraigne, D., Dehant, V., & Hinderer, J. 1994, J. Geophys. Res., 99, 9203 (erratum 100, 2041 [1995])
Dickey, J. O., et al. 1994, Science, 265, 482
Dones, L., & Tremaine, S. 1993, Science, 259, 350
Getino, J. 1995a, Geophys. J. Int., 120, 693
———. 1995b, Geophys. J. Int., 122, 803
Getino, J., & Ferrándiz, J. M. 2000, Geophys. J. Int., 142, 703
Greenspan, H. P. 1990, The Theory of Rotating Fluids (repr.; Brookline, MA: Breukelen)
Greff-Lefftz, M., & Legros, H. 1999, Science, 286, 1707
Goldreich, P., & Peale, S. J. 1970, AJ, 75, 273
Goldstein, H. 1980, Classical Mechanics (2d ed.; Reading, MA: Addison-Wesley)
Hartmann, W. K., & Vail, S. M. 1986, in Origin of the Moon, ed. W. K. Hartmann, R. J. Phillips, & G. J. Taylor (Houston: Lunar Planet. Inst.), 551
Hinderer, J., Legros, H., & Amalvict, M. 1987, Phys. Earth Planet. Inter., 49, 213
Hough, S. S. 1895, Philos. Trans. R. Soc. London, 186, 469
Kinoshita, H. 1977, Celest. Mech., 15, 277
Kinoshita, H., & Souchay, J. 1990, Celest. Mech. Dyn. Astron., 48, 187
Lamb, H. 1945, Hydrodynamics (6th ed.; New York: Dover)
Lambeck, K. 1980, The Earth's Variable Rotation (Cambridge: Cambridge Univ. Press)
Laskar, J. 1988, A&A, 198, 341
Lissauer, J. J. 1995, Icarus, 114, 217
Lissauer, J. J., & Safronov, V. S. 1991, Icarus, 93, 288
Mathews, P. M., Buffet, B. A., Herring, T. A., & Shapiro, I. I. 1991, J. Geophys. Res., 96, 8219
McKinnon, W. B., Zahnle, K. J., Ivanov, B. A., & Melosh, H. J. 1997, in Venus II, ed. S. W. Bougher, D. M. Hunten, & R. J. Philips (Tucson: Univ. Arizona Press), 969
Néron de Surgy, O., & Laskar, J. 1997, preprint
Plummer, H. C. 1962, An Introductory Treatise on Dynamical Astronomy (repr.; New York: Dover)
Poincaré, H. 1910, Bull. Astron., 27, 321
Ross, M. N., & Schubert, G. 1989, J. Geophys. Res., 94, 9533
Schaber, G. G., et al. 1992, in Papers Presented to the International Colloquium on Venus (LPI Contrib. 789) (Houston: Lunar Planet. Inst.), 100
Solomon, S. C., Bullock, M. A., & Grinspoon, D. H. 1999, Science, 286, 87
Sonett, C. P., Kvale, E. P., Zakharian, A., Chan, M. A., & Demko, T. M. 1996, Science, 273, 100
Strom, R. G., Schaber, G. G., & Dawson, D. D. 1994, J. Geophys. Res., 99, 10899
Toomre, A. 1966, in The Earth-Moon System, ed. B. G. Marsden & A. G. W. Cameron (New York: Plenum), 33
———. 1974, Geophys. J. RAS, 38, 335
Touma, J., & Wisdom, J. 1993, Science, 259, 1294
———. 1994a, AJ, 107, 1189 (TW94a)
———. 1994b, AJ, 108, 1943
———. 1998, AJ, 115, 1653
Williams, G. E. 1994, Earth Planet. Sci. Lett., 128, 155
Wisdom, J. 1985, Icarus, 63, 272
Wisdom, J., & Holman, M. 1991, AJ, 102, 1528
Yoder, C. F. 1995a, Icarus, 117, 250
———. 1995b, in Global Earth Physics, ed. T. J. Ahrens (Washington: Am. Geophys. Union), 1